Laser-stimulated fluorescence reveals unseen details in fossils from the Solnhofen Limestone (Upper Jurassic, Bavaria, Germany)

Luke Barlow (up812045@myport.ac.uk)
University of Portsmouth https://orcid.org/0000-0002-0867-649X
Michael Pittman
University of Hong Kong https://orcid.org/0000-0002-6149-3078
David Martill
University of Portsmouth
Thomas Kaye
Foundation for Scientific Advancement https://orcid.org/0000-0001-7996-618X
Anthony Butcher

Article

Keywords: Laser-Stimulated Fluorescence, ultraviolet, techniques, fluorescence, Jurassic, Solnhofen Limestone, Altmühtal Formation, Painten Formation, Mörnsheim Formation

Posted Date: August 24th, 2020

DOI: https://doi.org/10.21203/rs.3.rs-59716/v1

Abstract

Laser-Stimulated Fluorescence (LSF) has seen increased use in palaeontological investigations in recent years. The method uses the high flux of laser light to reveal details sometimes missed by ultraviolet (UV) and optical wavelengths. In this study, we compare the results of LSF with UV on a range of fossils from the Upper Jurassic Solnhofen Limestone Konservat-Lagerstätte of Bavaria, Germany. The methodology follows previous protocols with modifications made to enhance laser beam intensity. Our experiments show the value of LSF in revealing shallow subsurface detail of specimens, previously not widely applied to Solnhofen fossils. In particular, fossil decapods from the Solnhofen Limestone reveal full body outlines, even under the matrix, along with details of segmentation within the appendages such as limbs and antennae. The results indicate that LSF can be used on both vertebrate and invertebrate fossils and may surpass the information provided by traditional UV methods in some specimens.

Introduction

Since the introduction of ultraviolet (UV) fluorescence for the analysis of fossils from the Upper Jurassic Solnhofen Limestone lithographic limestones of Germany in the early 20th century (Miethe & Born 1928), the technique has been increasingly used in the analysis of exceptionally preserved fossils from this famous fossil Lagerstätte. Fossils from a wide range of phyla have been studied using UV including decapods (Schwiegert 2011), ammonites (Keupp 2007), fish (Tischlinger & Arratia 2013), pterosaurs (Frey *et al.* 2003) and dinosaurs (Göhlich & Chiappe 2006; Rauhut *et al.* 2012) among others. More recently, laser light techniques have been applied to fossils to induce fluorescence (Kaye *et al.* 2010), especially on 'iconic' fossil vertebrates from sites of exceptional preservation like *Anchiornis, Confuciusornis, Jianianhualong, Psittacosaurus* and *Sapeornis* (Vinther *et al.* 2016; Mayr *et al.* 2016; Xu *et al.* 2017; Kaye *et al.* 2019*a,b;* Pittman & Xu 2020; Serrano *et al.* 2020), including the first discovered fossil feather which is from the Solnhofen Limestone (Kaye *et al.* 2019*a).*. Fossils from the lithographic limestone horizons of the Solnhofen Limestone have been widely studied using UV and thus provides an ideal opportunity to compare the two fluorescent techniques on a range of fossils including cephalopods, decapods, and small vertebrates (Hess 1999; Zhou & Wang 2010) (Fig. 1). The Solnhofen Limestone is famous for its well-bedded, ultrafine-grained lithographic limestones (often called plattenkalk) and referred to as such herein) that formed in the calm basins of the Solnhofen lagoons on the northern margin of the Tethys Ocean (Viohl 1998; Munnecke *et al.* 2008). The palaeoenvironment represented by these limestones is a closed lagoonal system with high evaporation rates leading to a stratified water column with anoxic bottom waters largely devoid of macroorganisms (Viohl 1998). Occasional mixing through storms brought the toxic water to the aerated surface zone leading to the mass mortality of nektonic organisms (Pan *et al.* 2019). These organisms often became exceptionally well preserved due to a lack of scavenging, bacterial sealing, and rapid burial (Wellnhofer 2009). Here we compare images of Solnhofen fossils under LSF and UV and evaluate the use of LSF on fossils in this important Konservat-Lagerstätte.

Methods

The specimens used in this study labelled LB 1–13, abbreviated from the initials of the primary author, were collected during a series of field visits to the Solnhofen region over twenty years and are accessioned in the collection of the School of the Environment, Geography and Geosciences (SEGG), University of Portsmouth. Additional specimens from the Staatliche naturwissenschaftliche Sammlungen Bayerns, Bayerische Staatssammlung für Paläontologie und Geologie (SNSB-BSPG) were studied by MP and TGK during a visit to the Museum für Naturkunde (Kaye *et al.* 2019*a)* (Figs 13–16). The specimens used are based on availability and represent some of the main groups found in the Solnhofen Limestones.

Photography

Photographs were taken in a blacked-out room to avoid natural light contamination. An LED lamp illuminated the specimen obliquely (*c.* 45 degrees) or directly for the white light photographs.

The method of Laser-Stimulated Fluorescence modified from Kaye *et al. (*2015) used an MGL-III–532–1~300mW green diode-pumped solid-state (DPSS) laser with a PSU-III-LCD power supply with a set output of 85mW. Alterations to the method included mounting the laser onto a camera track where only a trucking motion was permitted, so the 532 nm green laser moved through the x-axis to scan the specimen whilst maintaining the same perpendicular relationship (Fig. 2). Through substituting trucking for the panning motion in previous publications, the laser module maintains a constant distance from the specimen and therefore a constant beam intensity across the entire fossil. For Figs 13–16 the same methodology was used in Kaye *et al.* 2019*a* with an abbreviated method stated here. A 1W 405nm blue laser was used to induce fluorescence and a Nikon DSLR was used to take the photographs with a 425nm blocking filter. Post-processing (equalisation, saturation, and colour balance) was then performed in Photoshop CS6.

The method of ultraviolet fluorescence consisted of a 365 nm lamp as used by Tischlinger & Frey (2002) with the specimen illuminated as close as possible.

The long-exposures for each image under all three lighting regimes were taken using a Nikon D5300 DSLR camera mounted on a tripod with a 2-second self-timer setting that prevents camera movement from affecting the image. Aperture priority mode controlled the length of exposure following the method described by Eklund *et al.* (2018). They suggested a 10 second exposure for UV and the ISO was adjusted accordingly. Using a low ISO prevents grainy photos and with a small aperture, other light sources are prevented from contaminating the image. 30 second exposures were used for imaging under LSF with the ISO left at 100. The position and distance of the specimen from the camera remained constant for each method so that LSF, white light, and UV images could be collected efficiently. This lighting sequence allowed the O56 blocking filter that prevents camera over-saturation with LSF to be applied effectively. This filter was removed for white light and UV photography, as although the filter can pick up UV

fluorescence, the fluorescence is clearer without a blocking filter. Due to the flattened nature of the fossils within Solnhofen laminites, repetitive photography and photo stacking techniques were unnecessary.

Health and Safety

It is important that when using LSF or UV techniques, appropriate safety precautions are observed. The green laser and UV lamp require laser and UV blocking goggles during operation and these methods were conducted in a locked room with a suitable exterior notice to prevent people from being harmed. Humans are most sensitive to green laser light (Galang *et al.* 2010) and by following these guidelines, the operators and others can be safeguarded. When using UV, 10-minute breaks were taken every 10–30 minutes to prevent eye damage and headaches (Tischlinger & Arratia 2013). Since pale colours fluoresce under UV light, dark clothing was worn while conducting scans.

Results

Cephalopoda

Cephalopods in the form of ammonites, belemnites and teuthoids occur frequently in the Solnhofen Limestone and are sometimes exceptionally well preserved (Fuchs *et al.* 2015). Many have been reported with aspects of their soft tissues preserved, including impressions of tentacles with hooklets in belemnites and teuthoids (Klug *et al.* 2016), the musculature of the mantle in teuthoids (Klug *et al.* 2015) and the siphuncle and pellicula in ammonites (Keupp 2007). Although ammonites make up a large portion of the fossils from the Solnhofen plattenkalks, they are often poorly preserved due to the aragonitic composition of the shell which is readily dissolved during diagenesis (Seilacher *et al.* 1976). This dissolution leaves behind an external or composite mould in the matrix, occasionally with the original outline and the calcitic aptychi in the body chamber (Keupp 2007).

Although rarely preserved, the original shell can be observed once replaced by calcite in the phragmacone (Fig. 4) and the body chamber (Arratia *et al.* 2015). The body chamber is present within the halo of the dissolved shell and can be enhanced under UV and LSF (Fig. 6). The siphuncle, pellicula and other non-mineralised elements are often phosphatised in Solnhofen ammonites and these may fluoresce more intensely than the remaining shell (Keupp 2007). UV fluorescence displays colour differences on these ammonites (Fig. 6C), but the contrast between non-mineralised parts and the surrounding shell is lacking, when compared with the LSF image of specimen LB 4 (Fig. 6D). It appears that the raised darker areas on isolated aptychi (LB 1) (Fig. 3) are the thick spongy layer on the inside of the aptychus underlying the thinner crenulated outer layer, rather than soft tissues following Lehmann (1976).

Lumbricaria Goldfuss, 1831, a coprolite attributed to ammonites (Janicke 1970) lies on the same slab as an ammonite (Fig. 6) and appears to contain aptychi of a smaller ammonite. *Plesioteuthis prisca (*Rüppell, 1829), a squid from the Solnhofen Limestone with a central rachis that is revealed in its entirety

and fluoresces at two distinct levels under LSF (Fig. 7D). This rachis runs along the centre of the visible body outline, although no soft tissues of the mantle are present (Fig. 7).

Decapoda

Decapod crustacea occur frequently in the Solnhofen plattenkalks and are often well preserved as fully articulated individuals, even in the larval stage (Haug *et al.* 2008; Winkler 2014). The fossils are valuable for understanding arthropod ontogeny, with specimens that display growth cycles only known from a few other Lagerstätten (J. T. Haug *et al.* 2009). Numerous studies have been carried out using UV fluorescence, revealing unseen details to allow distinctions between taxa or increasing the specimen-matrix contrast (Haug *et al.* 2011; Winkler 2012; Audo *et al.* 2014). The decapods lend themselves to techniques using fluorescence as they hold autofluorescent compounds within their exoskeleton (Haug *et al.* 2011; Glenn *et al.* 2013).

The preservation of the fossils studied (LB 6–9), vary from isolated appendages to complete articulated examples. A single walking leg attributed to *Aeger tipularius* von Schlotheim, 1822 (Fig. 8) is near complete with only a few setae missing from the exposed surface. UV fluorescence enhances the specimen-matrix contrast but fails to fluoresce below the matrix where the complete setae are revealed through LSF (Fig. 8).

Anatomical details of complete specimens of *Cycleryon propinquus* von Schlotheim, 1822 (Fig. 9) and *Antrimpos speciosus* Münster, 1839 (Figs 10, 11) are enhanced through fluorescent techniques as previous studies demonstrate (Schweigert & Garassino 2004). However, it must be reiterated that previous studies on Solnhofen material have only used ultraviolet as a means of fluorescence (Keupp 2007; Schweigert 2011; Tischlinger & Arratia 2013). A distal portion of the left first pereiopod on LB 7 is unseen under UV light but is revealed, albeit faintly, under LSF (Fig. 8). In *Antrimpos speciosus (*LB 8) *(*Figs 10–11), more detail of the body outline is exposed by LSF under a green 532 nm laser compared with UV and this is emphasised in the magnified portions (Figs 9, 10 B-C, E-F).

As the figures of Solnhofen decapods herein show, the detail revealed under Laser-Stimulated Fluorescence, often surpasses that revealed by ultraviolet fluorescence, with the outline of the entire animal outline being revealed, along with small elements such as antennae and swimmerets (Figs 10, 11). The veneer of the matrix on LB 8 in Figs 10–11 may have obstructed the UV fluorescence and could be prepared further to assist the use of this method. Ultraviolet fluorescence on a specimen of *Alcmonacaris winkleri* Polz, 2008 (LB 9) reveals a faint outline of the animal while recording colour patterning (Fig. 12). Under LSF, green laser light, this colour information is lost but the animal is revealed in its entirety (Fig. 12D). Techniques to rectify this loss of information have been developed using multiple wavelengths (Kaye *et al.* 2015). As Figs 9–12 show, the preserved exoskeleton and the body outline fluoresce at different levels because of the autofluorescent compounds within the arthropod exoskeleton.

Vertebrata

The Solnhofen Limestone has achieved much of its fame as a fossil Konservat-Lagerstätten because of the exceptional preservation of its vertebrate fossils, especially those of volant animals such as the earliest unequivocal fossil bird *Archaeopteryx* and a diverse assemblage of pterosaurs (Beardmore *et al.* 2017; Schwarz *et al.* 2019; Longrich *et al.* 2020) where parts of the flight surfaces are preserved, including wing membranes and feathers (Frey *et al.* 2003; Jäger *et al.* 2018; Benton *et al.* 2019; Kaye *et al.* 2019*a;* Foth *et al.* 2020; Wilkin 2020). Some of this exceptional preservation can be seen in the examples below (Figs 13–16). The hollow bones of pterosaurs are rarely preserved and through LSF the contrast between preserved bone and the imprints of the skeleton in the matrix is exemplified. The dwarf crocodilyform *Alligatorellus (*Fig. 16) under the blue laser displays soft tissues around the entire body as well as a brighter section at the base of the tail that may represent partial preservation of the caudofemoralis muscle.

However, the exceptional preservation is not restricted to the Tetrapoda, with many fishes also exceptionally well preserved with full articulation and soft part preservation (Konwert 2016; Arratia *et al.* 2019; Ebert & Lane 2019) as well as reptiles (Tennant & Mannion, 2014) (see Fig. 17). Specimens LB 10–13 (Figs 17–20) vary in completeness from articulated individuals to isolated sources of phosphate, resulting in the high level of fluorescence under UV and LSF (Fig. 12).

The specimens studied vary between right and left lateral views, seen in specimens LB 10 and 11 (Figs 17 and 18 respectively). The fluorescence of these specimens (LB 10–13), results from the vertebrate endoskeleton containing high levels of phosphorus (Tischlinger & Arratia 2013). The fossils in white light contrast little with the surrounding sediment as in many other Solnhofen fossils. Indeed, it may be difficult to see some fossils, especially when weathered, without using fluorescence.

Many Solnhofen fossil fish possess a fully ossified skull, fins, neural and haemal spines made apparent through fluorescence along with thin autocentra (Arratia & Schultze 2013). The autocentra surrounding the dark chordocentra are thin and almost translucent and fluoresce under both UV and LSF. Species of the teleost family Orthogonikleithridae are the most common vertebrates in the Solnhofen Limestones (Konwert 2016). The ossification patterns observed on a specimen of *Orthogonikleithrus hoelli* Arratia, 1997 (LB 12) (Fig. 19), correspond with previous studies using UV for fluorescence (Tischlinger & Arratia 2013).

Fish fluoresce well under both UV and LSF and although the difference is often minimal, clearly in Fig. 18 LSF surpasses the UV photograph with an increased fluorescence of both the skull and vertebral column completing the structures seen and this results from the higher flux and subsurface illumination.

Discussion

Laser-Stimulated Fluorescence has various applications as illustrated by the numerous examples figured by Kaye et al. (2015) including an automated microvertebrate sorting machine developed to reduce time

spent on manual sorting along with demonstrating the potential of LSF to reveal subsurface fossils (Kaye *et al.* 2015, Figs 10 and 8 respectively). Recently, it has even been applied as part of an automated drone system to seek out fossils on the ground at night (Kaye & Pittman 2020). The technique has revealed geochemical halos around the lost calamus of '*Archaeopteryx'* (Kaye *et al.* 2019*b*)„ akin to the effect observed in Figs 10–12 where the fluorescence of decapods extends beyond the preserved exoskeleton. The methodology is simple and provides a rapid means for producing high-quality images of fluorescing fossils, allowing for a camera image to be available within 30 seconds of exposure. This exposure time is longer than UV or white light photography as the fluorescence occurs through a fine laser beam scanning an entire specimen rather than the instant illumination under an LED or UV lamp. The same wavelengths of 532nm have been employed previously (Kaye *et al.* 2015), although this green light is often substituted for blue or violet wavelengths (T. Kaye, pers. comm. 2019). Blue/violet lasers increase the contrast further and reveal fluorescence colour differences akin to those under UV (Schwarz *et al.* 2019). The 532nm laser in this study results in varying levels of orange fluorescence through the O56 blocking filter that can cause difficulties in distinguishing between different parts of a specimen. As reported by several studies (Mayr *et al.* 2016; Vinther *et al.* 2016; Wang *et al.* 2017; Saitta *et al.* 2018, Falk *et al.* 2019; Yang *et al.* 2019; Pittman & Xu 2020; Serrano *et al.* 2020), LSF continues to reveal new and exciting details on well-preserved fossil assemblages (Konservat-Lagerstätten) like the Jehol Lagerstätte of northeastern China and the Las Hoyas Lagerstätte of Spain. The high fluorescence we observed in decapods (Figs 8–12) likely results from the autofluorescence present in crustacean exoskeletons (Charbonnier *et al.* 2017). The Solnhofen specimens analysed here fluoresce brightly due to high levels of phosphate in both original and diagenetic minerals (Wilby *et al.* 1996). The principal findings in the Solnhofen specimens are that LSF reveals morphology not visible under other UV techniques and more often to a greater degree of clarity and depth.

Costs

With reductions to the cost of laser systems, the method could be replicated using a 532nm laser, an LCD power supply and a Zecti 31.5in”/80cm camera slider. This study using an 85mW laser shows the technique can be used with less powerful laser equipment than the 300–500mW laser used by Falk *et al.* (2016) and Wang *et al.* (2017). With two wavelengths in tandem, different structures fluoresce, allowing for a more complete picture (Wang *et al.* 2017), providing an option for further research. The use of a less powerful laser also allows for LSF to be more accessible on the grounds of cost, but with a necessary trade-off in fluorescence signal.

Conclusions

The list of non-destructive techniques available to palaeontologists is increasing. X-rays were first implemented in 1896 on fossils from another German Lagerstätte, the Devonian Hunsrück Slate (Hohenstein 2004), and was widely implemented from the 1930s by Lehmann on this site along with other fossil-rich areas like Messel pit and the Solnhofen region. The use of UV has become standard in

many palaeontological studies especially those investigating soft tissue preservation (Hone et al. 2010; Kellner et al. 2010; Cuesta et al. 2015; Schwarz et al. 2019; Hoffman et al. 2020) since its first use in 1926 on fossil vertebrates within the Solnhofen plattenkalks (Simpson 1926). Composite imaging and 3D computer modelling have also been used on Solnhofen fossils and provide a valuable alternative, especially on small and delicate specimens (Haug *et al.* 2008). Synchrotron Rapid Scanning X-ray Fluorescence (SRS-XRF) combined with chemical images allowed for the mapping of plumage patterns in the iconic Solnhofen bird *Archaeopteryx* (Manning *et al.* 2013).

LSF was added to the literature as recently as 2015. The use of lower-powered equipment in this study illustrates that the technique can still be employed to good effect and could provide a valuable teaching resource. The method can be performed in as little as 30 seconds, allowing for almost instant data collection. Previous publications have focused entirely on vertebrate material. This study shows the effect of LSF on invertebrates for the first time. In addition, it adds the Solnhofen plattenkalks to the list of Konservat-Lagerstätten where the effects under LSF are now known. This study underscores LSF as an alternative tool to UV for non-destructive palaeontological investigation using extensive comparative figures that show unseen details to an equal and often greater extent than UV.

Declarations

Acknowledgements

MP and TGK's participation in this study was supported by the RAE Improvement Fund of the Faculty of Science, The University of Hong Kong (HKU) and funds from the HKU MOOC Dinosaur Ecosystems. MP was also supported by Research Grant Council General Research Fund 17103315. TGK was also supported by the Foundation for Scientific Advancement. We would like to thank Oliver Rauhut for granting us access to specimens in his care at the Bavarian State Collections of Palaeontology and Geology.

References

1. ARRATIA, G. 1997. Basal teleosts and teleostean phylogeny. *Palaeo Ichthyologica*, **7**, 1-168.
2. — and SCHULTZE, H. P. and TISCHLINGER, H. 2019. On a remarkable new species of *Tharsis*, a Late Jurassic teleostean fish from southern Germany: its morphology and phylogenetic relationships. *Fossil Record*, **22**(1), 23 pp.
3. — and SCHULTZE, H., TISCHLINGER, H. and VIOHL, G. 2015. *Solnhofen - ein fenster in die Jurazeit 1+2 - gesamtausgabe*. 1st edn. Verlag Friedrich Pfeil, Munchen, 607 pp.
4. AUDO, D. and CHARBONNIER, S. 2012. Late Cretaceous crest-bearing shrimps from the Sahel Alma Lagerstätte of Lebanon. *Acta Palaeontologica Polonica*, **58**(2), 335-349.
5. — and SCHWEIGERT, G., HAUG, J. T., HAUG, C., SAINT MARTIN, J. P. and CHARBONNIER, S. 2014. Diversity and palaeoecology of the enigmatic genus *Knebelia* (Eucrustacea, Decapoda, Eryonidae)

from Upper Jurassic plattenkalks in southern Germany. *Palaeontology*, **57**(2), 397-416.

6. BARTELS, C. 2009. *The fossils of the Hunsruck slate: Marine life in the Devonian*. 2nd edn. Cambridge University Press, Cambridge, UK, 86–88.
7. BEARDMORE, S. R., LAWLOR, E. and HONE, D. W. E. 2017. Using taphonomy to infer differences in soft tissues between taxa: an example using basal and derived forms of Solnhofen pterosaurs. *The Science of Nature*, **104**(7-8), 65 pp.
8. BENTON, M. J., DHOUAILLY, D., JIANG, B. and MCNAMARA, M. 2019. The early origin of feathers. *Trends in ecology & evolution*, **34**, 856-869.
9. BLAINVILLE, H.D. 1818. Poissons fossils. *Nouveau Dictionnaire d'Histoire Naturelle*, Nouvelle édition Chez Deterville, **27**, 319–359.
10. CHARBONNIER, S., AUDO, D., GARASSINO, A. and HYŽNÝ, M. 2017. *Fossil crustacea of Lebanon*. Publications Scientifiques du Muséum, Paris, 252 pp.
11. CONROY, G. C. and VANNIER, M. W. 1984. Noninvasive three-dimensional computer imaging of matrix-filled fossil skulls by high-resolution computed tomography. *Science*, **226**(4673), 456-458.
12. CUESTA, E., DIAZ-MARTINEZ, I., ORTEGA, F. and SANZ, J. L. 2015. Did all theropods have chicken-like feet? First evidence of a non-avian dinosaur podotheca. *Cretaceous Research*, **56**, 53-59.
13. EBERT, M. 2019. *Zandtfuro* and *Schernfeldfuro*, New Genera of Halecomorphi (Actinopterygii) from the Upper Jurassic Solnhofen Archipelago. *Journal of Vertebrate Paleontology*, **39**(2). doi: 10.1080/02724634.2019.1592759
14. — and KÖLBL-EBERT, M. and LANE, J. A. 2015. Fauna and predator-prey relationships of Ettling, an actinopterygian fish-dominated Konservat-Lagerstätte from the Late Jurassic of southern Germany. *PLoS One*, **10**(1). doi: 10.1371/journal.pone.0116140
15. EKLUND, M. J., AASE, A. K. and BELL, C.J. 2018. Progressive Photonics: methods and applications of sequential imaging using visible and non-visible spectra to enhance data-yield and facilitate forensic interpretation of fossils. *Journal of Paleontological Techniques*, **20**, 1-36.
16. FALK, A. R., KAYE, T. G., ZHOU, Z. and BURNHAM, D. A. 2016. Laser fluorescence illuminates the soft tissue and life habits of the Early Cretaceous bird *Confuciusornis*. *PLoS One*, **11**(12). doi: 10.1371/journal.pone.0167284
17. — and O'CONNOR, J., WANG, M. and ZHOU, Z. 2019. On the preservation of the beak in *Confuciusornis* (Aves: Pygostylia). *Diversity*, **11**(11), 212 pp. doi: 10.3390/d11110212
18. FOTH, C., HAUG, C., HAUG, J. T., TISCHLINGER, H. and RAUHUT, O. W. 2020. Two of a feather: a comparison of the preserved integument in the juvenile theropod dinosaurs *Sciurumimus* and *Juravenator* from the Kimmeridgian Torleite Formation of southern Germany. In *The Evolution of Feathers*. Springer, Cham, 79-101.
19. FREY, E., TISCHLINGER, H., BUCHY, M. C. and MARTILL, D. M. 2003. New specimens of Pterosauria (Reptilia) with soft parts with implications for pterosaurian anatomy and locomotion. *Geological Society, London, Special Publications*, **217**(1), 233-266.

20. GALANG, J., RESTELLI, A., HAGLEY, E. W. and CLARK, C. W. 2010. A red light for green laser pointers. *Optics and Photonics News*, **21**(10), 11-13.
21. GLENN, D., PAKES, M. J. and CALDWELL, R. L. 2013. Fluorescence in Arthropoda informs ecological studies in anchialine crustaceans, Remipedia, and Atyidae. *Journal of Crustacean Biology*, **33**(5), 620-626.
22. GÖHLICH, U. B. and CHIAPPE, L. M. 2006. A new carnivorous dinosaur from the Late Jurassic Solnhofen archipelago. *Nature*, **440**, 329-332.
23. GOLDFUSS, A. 1831. *Petrefacta Germaniae - Abbildungen und Beschreibungen der Petrefacten Deutschlands und der angränzenden Länder. Erster Theil.* Arnz and Company, Dusseldorf, 1-252.
24. HAUG, C., HAUG, J. T., WALOSZEK, D., MAAS, A., FRATTIGIANI, R. and LIEBAU, S. 2009. New methods to document fossils from lithographic limestones of southern Germany and Lebanon. *Palaeontologia Electronica*, **12**(3), 12 pp.
25. HAUG, J. T., HAUG, C. and EHRLICH, M. 2008. First fossil stomatopod larva (Arthropoda: Crustacea) and a new way of documenting Solnhofen fossils (Upper Jurassic, Southern Germany). *Palaeodiversity*, **1**, 103-109.
26. — and HAUG, C., WALOSZEK, D., MAAS, A., WULF, M. and SCHWEIGERT, G. 2009. Development in Mesozoic scyllarids and implications for the evolution of Achelata (Reptantia, Decapoda, Crustacea). *Palaeodiversity*, **2**, 97-110.
27. — and HAUG, C., KUTSCHERA, V., MAYER, G., MAAS, A., LIEBAU, S., CASTELLANI, C., WOLFRAM, U., CLARKSON, E. N. K. and WALOSZEK, D. 2011. Autofluorescence imaging, an excellent tool for comparative morphology. *Journal of Microscopy*, **244**(3), 259-272.
28. HILL, C. R. 1990. Scanning electron microscopy in palaeobotany. *Scanning Electron Microscopy in Taxonomy and Functional Morphology. Systematics Association Special Volume Series,* **41**, 193-234.
29. HOFFMANN, R., BESTWICK, J., BERNDT, G., BERNDT, R., FUCHS, D. and KLUG, C. 2020. Pterosaurs ate soft-bodied cephalopods (Coleoidea). *Scientific Reports*, **10**(1), 1-7.
30. HOHENSTEIN, P. 2004. X-ray imaging for palaeontology. *The British Journal of Radiology*, **77**(917), 420-425.
31. HONE, D. W., TISCHLINGER, H., XU, X. and ZHANG, F. 2010. The extent of the preserved feathers on the four-winged dinosaur *Microraptor gui* under ultraviolet light. *PloS one*, **5**(2). doi: 10.1371/journal.pone.0009223
32. JÄGER, K. R., TISCHLINGER, H., OLESCHINSKI, G. and SANDER, P. M. 2018. Goldfuss was right: Soft part preservation in the Late Jurassic pterosaur *Scaphognathus crassirostris* revealed by reflectance transformation imaging and ultraviolet light and the auspicious beginnings of paleo-art. *Palaeontologia Electronica*, **21**(3). doi 10.26879/713
33. JANICKE, V. 1970. *Lumbricaria*, ein cephalopoden–koprolith. *Neues Jahrbuch für Geologie und Paläontologie, Monatshefte*, **1**, 50-60.
34. KAYE, T. G. and PITTMAN, M. 2020. Fluorescence-based detection of field targets using an autonomous unmanned aerial vehicle system. *Methods in Ecology and Evolution*. doi:

10.1111/2041-210X.13402

35. — and MARTIN, L., BURNHAM, D. and GONG, E. 2010. Multispectral imaging and analysis of a Liaoning 'mystery specimen'. In *70th Annual Meeting of the Society of Vertebrate Paleontology*.
36. — and FALK, A. R., PITTMAN, M., SERENO, P. C., MARTIN, L. D., BURNHAM, D. A., GONG, E., XU, X. and WANG, Y. 2015. Laser-stimulated fluorescence in paleontology. *PloS one*, **10**(5). doi: 10.1371/journal.pone.0125923
37. — and PITTMAN, M., MAYR, G., SCHWARZ, D. and XU, X. 2019*a*. Detection of lost calamus challenges identity of isolated *Archaeopteryx* feather. *Scientific reports*, **9**(1), 1-6.
38. — and PITTMAN, M., MARUGÁN-LOBÓN, J., MARTÍN-ABAD, H., SANZ, J. L. and BUSCALIONI, A. D. 2019*b*. Fully fledged enantiornithine hatchling revealed by laser-stimulated fluorescence supports precocial nesting behaviour. *Scientific reports*, **9**(1), 1-4.
39. KELLNER, A. W., WANG, X., TISCHLINGER, H., DE ALMEIDA CAMPOS, D., HONE, D. W. and MENG, X. 2010. The soft tissue of *Jeholopterus* (Pterosauria, Anurognathidae, Batrachognathinae) and the structure of the pterosaur wing membrane. *Proceedings of the Royal Society B: Biological Sciences*, **277**(1679), 321-329.
40. KEUPP, H. 2007. Complete ammonoid jaw apparatuses from the Solnhofen plattenkalks: implications for aptychi function and microphagous feeding of ammonoids. *Neues Jahrbuch für Geologie und Paläontologie-Abhandlungen*, **245**(1), 93-101.
41. — and RIEDEL, F. 2010. Remarks on the possible function of the apophyses of the Middle Jurassic microconch ammonite *Ebrayiceras sulcatum* (Zieten, 1830), with a discussion on the palaeobiology of Aptychophora in general. *Neues Jahrbuch für Geologie und Paläontologie-Abhandlungen*, **255**(3), 301-314.
42. KLUG, C., FUCHS, D., SCHWEIGERT, G., RÖPER, M. and TISCHLINGER, H. 2015. New anatomical information on arms and fins from exceptionally preserved *Plesioteuthis* (Coleoidea) from the Late Jurassic of Germany. *Swiss Journal of Palaeontology*, **134**(2), 245-255.
43. — and SCHWEIGERT, G., FUCHS, D., KRUTA, I. and TISCHLINGER, H. 2016. Adaptations to squid-style high-speed swimming in Jurassic belemnitids. *Biology letters*, **12**(1). doi 10.1098/rsbl.2015.0877
44. KONWERT, M. 2016. *Orthogonikleithrus francogalliensis*, sp. nov. (Teleostei, Orthogonikleithridae) from the Late Jurassic Plattenkalks of Cerin (France). *Journal of Vertebrate Paleontology*, **36**(3), 1-10.
45. KOWALSKI, J., BODZIOCH, A., JANECKI, P. A., RUCIŃSKI, M. R. and ANTCZAK, M. 2019. Preliminary report on the microvertebrate faunal remains from the Late Triassic locality at Krasiejów, SW Poland. *Annales Societatis Geologorum Poloniae*, **89**(3), 291-305.
46. LEHMANN, U. 1976. *Ammonites: their lives and their environment*. Enke Verlag, Stuttgart, 171 pp.
47. LONGRICH, N. R., TISCHLINGER, H. and FOTH, C. 2020. The Feathers of the Jurassic Urvogel *Archaeopteryx*. In *The Evolution of Feathers*. Springer, Cham, 119-146.
48. MANNING, P. L., EDWARDS, N. P., WOGELIUS, R. A., BERGMANN, U., BARDEN, H. E., LARSON, P. L., SCHWARZ-WINGS, D., EGERTON, V. M., SOKARAS, D., MORI, R. A. and SELLERS, W. I. 2013.

Synchrotron-based chemical imaging reveals plumage patterns in a 150 million year old early bird. *Journal of Analytical Atomic Spectrometry*, **28**(7), 1024-1030.

49. MAYR, G., PITTMAN, M., SAITTA, E., KAYE, T. G. and VINTHER, J. 2016. Structure and homology of *Psittacosaurus* tail bristles. *Palaeontology*, **59**(6), 793-802.
50. MIETHE, A. and BORN, A. 1928. Die fluorographie von fossilien. *Paläontologische Zeitschrift*, **9**(4), 343-356.
51. MUNNECKE, A., WESTPHAL, H. and KÖLBL-EBERT, M. 2008. Diagenesis of plattenkalk: examples from the Solnhofen area (Upper Jurassic, southern Germany). *Sedimentology*, **55**(6), 1931-1946.
52. MÜNSTER, G. V. 1839. Decapoda Macroura. Abbildung und Beschreibung der fossilen langschwiinzigen Krebse in den Kalkschiefern von Bayern. *Beitraege zur Petrefactenkunde*, **2**, 1-88.
53. OPPEL A. 1863. Über jurassische Cephalopoden, *Palaeontologische Mittheilungen aus dem Museum des königlich Bayerischen Staates*, **3**, 163- 266.
54. PAN, Y., FÜRSICH, F. T., CHELLOUCHE, P. and HU, L. 2019. Taphonomy of fish concentrations from the Upper Jurassic Solnhofen Plattenkalk of Southern Germany. *Neues Jahrbuch für Geologie und Paläontologie-Abhandlungen*, **292**(1), 73-92.
55. PARENT, H. and WESTERMANN, G. E. 2016. Jurassic ammonite aptychi: functions and evolutionary implications. *Swiss Journal of Palaeontology*, **135**(1), 101-108.
56. **PITTMAN, M.** and XU, X. (editors). 2020. Pennaraptoran theropod dinosaurs: past progress & new frontiers. *Bulletin of the American Museum of Natural History*, 320 pp, in press.
57. POLZ H. 2008. *Alcmonacaris winkleri* g. nov. sp. nov. (Crustacea: Decapoda: Pleocyemata: Caridea) aus den Solnhofener Plattenkalken von Eichstätt. *Archaeopteryx*, **26**, 1–9.
58. RACICOT, R. 2016. Fossil secrets revealed: X-ray CT scanning and applications in paleontology. *The Paleontological Society Papers*, **22**, 21-38.
59. RAUHUT, O. W., FOTH, C., TISCHLINGER, H. and NORELL, M. A. 2012. Exceptionally preserved juvenile megalosauroid theropod dinosaur with filamentous integument from the Late Jurassic of Germany. *Proceedings of the National Academy of Sciences*, **109**(29), 11746-11751.
60. RÜPPELL, E. 1829. *Abbildung und Beschreibung einiger neuer oder wenig bekannten Versteinerungen aus der Kalkschieferformation von Solnhofen*. Brönner Verlag, Frankfurt, 12 pp.
61. SAITTA, E. T., FLETCHER, I., MARTIN, P., PITTMAN, M., KAYE, T. G., TRUE, L. D., NORELL, M.A., ABBOTT, G. D., SUMMONS, R. E., PENKMAN, K. and VINTHER, J. 2018. Preservation of feather fibers from the Late Cretaceous dinosaur *Shuvuuia deserti* raises concern about immunohistochemical analyses on fossils. *Organic Geochemistry*, **125**, 142-151.
62. SCHLOTHEIM, E.F. VON. 1822. *Nachtrage zur Petrefacktenkunde*. Becker, Gotha, 114 pp.
63. SCHWARZ, D., KUNDRÁT, M., TISCHLINGER, H., DYKE, G. and CARNEY, R. M. 2019. Ultraviolet light illuminates the avian nature of the Berlin *Archaeopteryx* skeleton. *Scientific reports*, **9**(1), 1-11.
64. SCHWEIGERT, G. 2011. The decapod crustaceans of the Upper Jurassic Solnhofen Limestones: a historical review and some recent discoveries. *Neues Jahrbuch für Geologie und Paläontologie-*

Abhandlungen, **260**(2), 131-140.

65. — and GARASSINO, A. 2004. *New genera and species of shrimps (Crustacea: Decapoda: Dendrobranchiata, Caridea) from the Upper Jurassic lithographic limestones of S. Germany*. Stuttgarter Beiträge zur Naturkunde, Staatliches Museum für Naturkunde, Rosenstein 1, D-70191 Stuttgart, **350**, 33 pp.
66. SEILACHER, A., ANDALIB, F., DIETL, G. and GOCHT, H. 1976. Preservational history of compressed Jurassic ammonites from southern Germany. *Neues Jahrbuch für Geologie und Paläontologie, Abhandlungen*, **152**, 307-356.
67. SERRANO, F. J., PITTMAN, M., KAYE, T.G., WANG, X.L., ZHENG, X.T. and CHIAPPE, L.M. 2020. Laser-Stimulated Fluorescence refines flight modelling of the Early Cretaceous bird *Sapeornis*.
68. STÜRMER, W., SCHAARSCHMIDT, F. and MITTMEYER, H. 1980. *Versteinertes Leben Im Röntgenlicht*. W. Kramer, Frankfurt am Main, 80 pp.
69. SYLVESTER-BRADLEY, P. C. 1969. Aluminum Coating in Scanning Electron Microscopy. *Micropaleontology*, **15**(3), 366 pp.
70. TISCHLINGER, H. and ARRATIA, G. 2013. Ultraviolet light as a tool for investigating Mesozoic fishes, with a focus on the ichthyofauna of the Solnhofen archipelago. *Mesozoic fishes*, **5**, 549-560.
71. — and FREY, E. 2002. Ein *Rhamphorhynchus* (Pterosauria, Reptilia) mit ungewöhnlicher Flughauterhaltung aus dem Solnhofener Plattenkalk. *Archaeopteryx*, **20**, 1-20.
72. VINTHER, J., NICHOLLS, R., LAUTENSCHLAGER, S., PITTMAN, M., KAYE, T. G., RAYFIELD, E., MAYR, G. and CUTHILL, I. C. 2016. 3D camouflage in an ornithischian dinosaur. *Current Biology*, **26**(18), 2456-2462.
73. VIOHL, G. 1998. The Solnhofen lithographic limestone - genesis and habitats. *Archaeopteryx*, **16**, 37-68.
74. WANG, X., PITTMAN, M., ZHENG, X., KAYE, T. G., FALK, A. R., HARTMAN, S. A. and XU, X. 2017. Basal paravian functional anatomy illuminated by high-detail body outline. *Nature communications*, **8**, 1-6.
75. WELLNHOFER, P. 2009. *Archaeopteryx: the icon of evolution.* Verlag Friedrich Pfeil, Munchen, 208 pp.
76. WILBY, P. R., BRIGGS, D. E., BERNIER, P. and GAILLARD, C. 1996. Role of microbial mats in the fossilization of soft tissues. *Geology*, **24**(9), 787-790.
77. WILKIN, J. 2020. The south German Plattenkalks. *Geology Today*, **36**(1), 27-32.
78. WINKLER, N. 2012. *Libanocaris annettae* nov. sp. (Crustacea: Dendrobranchiata: Penaeidae) from the Upper Jurassic Solnhofen Lithographic Limestones of Eichstätt. *Zitteliana*, 59-65.
79. WINKLER, N. 2014. A new caridean shrimp (Crustacea: Decapoda: Dendrobranchiata) from the Upper Jurassic Solnhofen Lithographic Limestones of Schernfeld (South Germany). *Zitteliana*, 83-90.
80. XU, X., CURRIE, P., PITTMAN, M., XING, L., MENG, Q., LÜ, J., HU, D. and YU, C. 2017. Mosaic evolution in an asymmetrically feathered troodontid dinosaur with transitional features. *Nature Communications*, **8**(1), 1-12.

Figures

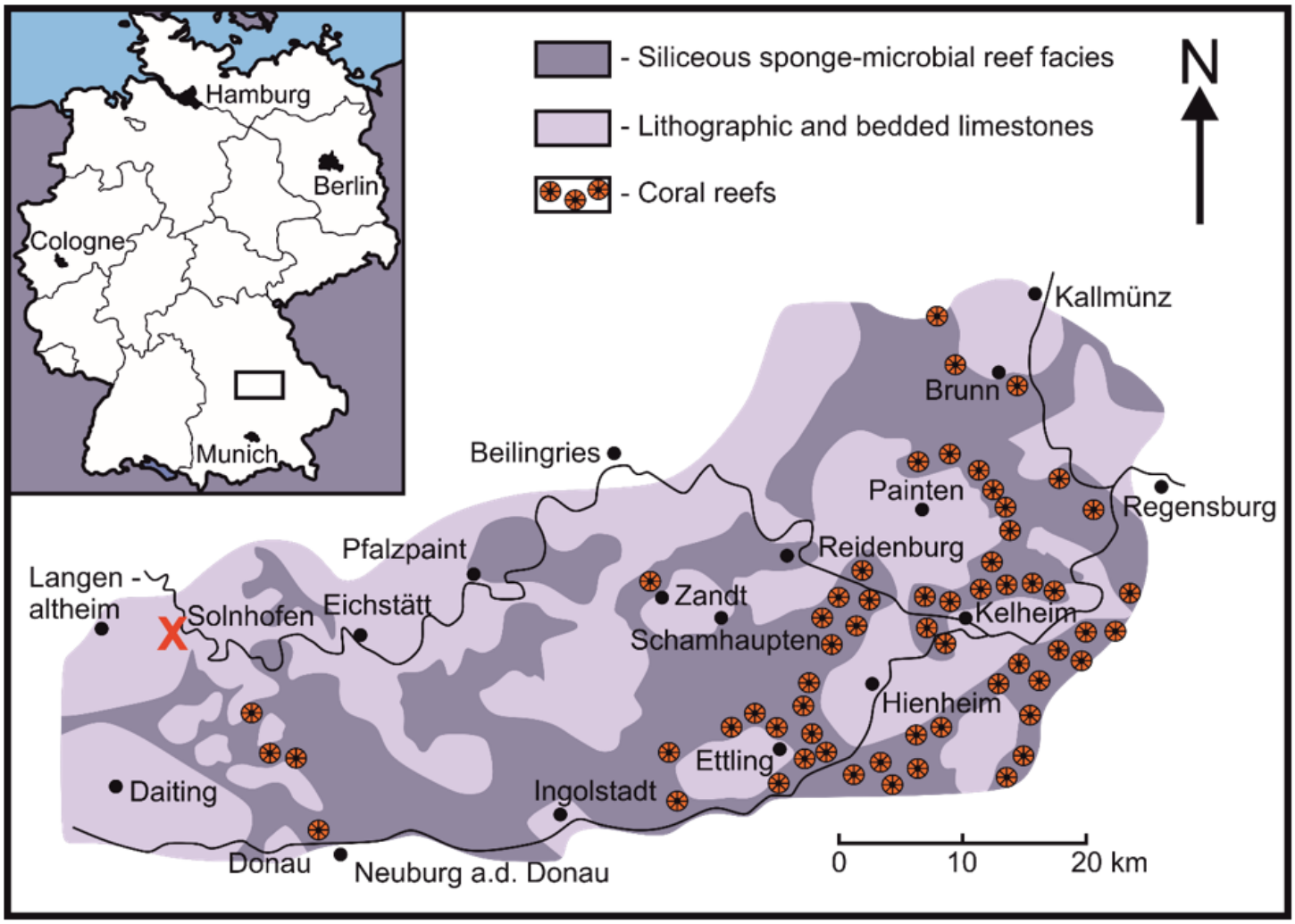

Figure 1

A facies map of the Solnhofen Limestones in Bavaria, southern Germany with the location X indicates the source of the fossils used in this study. Modified from Ebert et al. (2015).

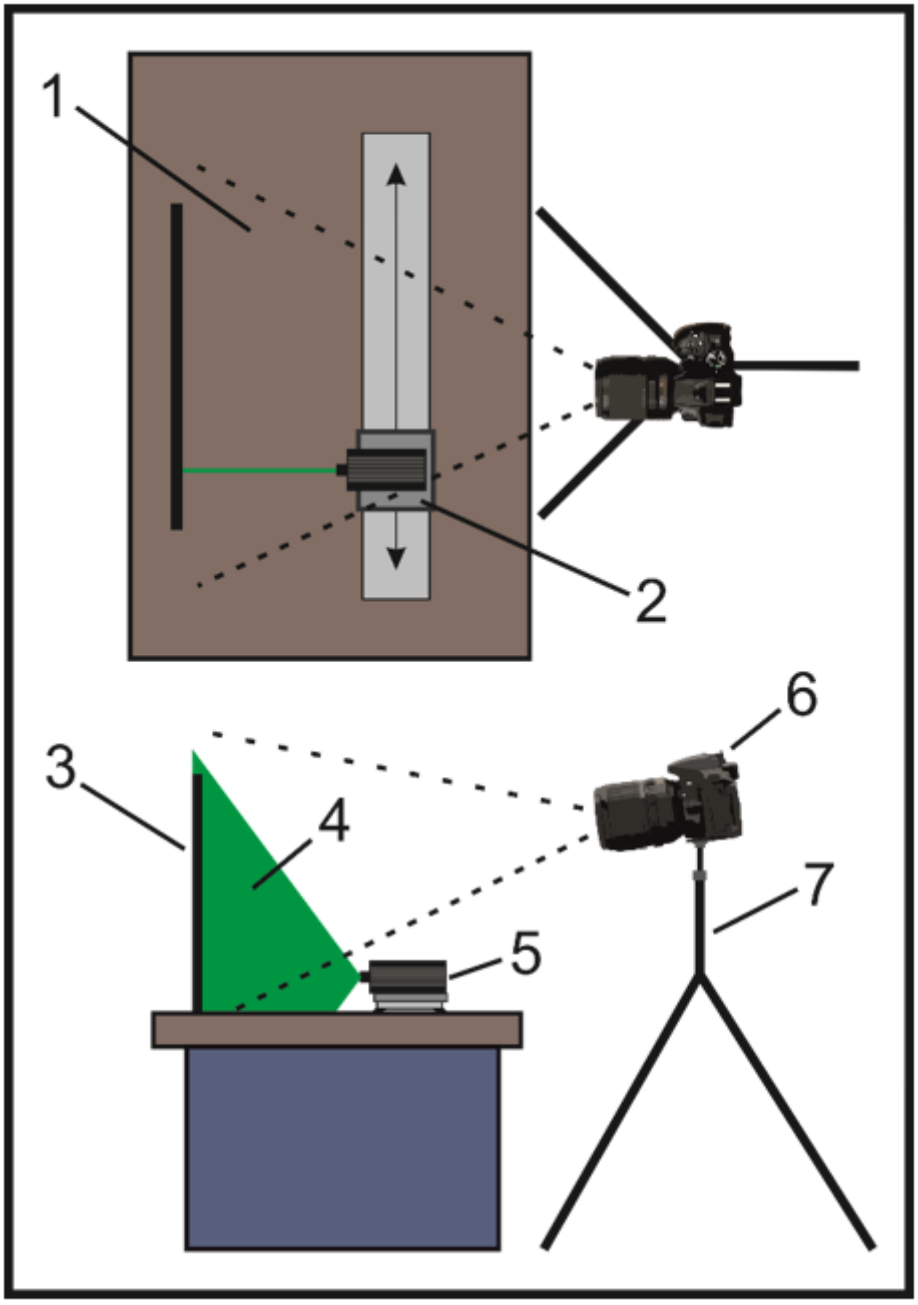

Figure 2

A simplified diagram of the camera and specimen table setup used to perform LSF imaging. 1, The image area of the DSLR camera; 2, Carriage of the camera track holding the laser module; 3, The imaged specimen; 4, Laser illumination using a line generator; 5, 85mW 532nm laser module; 6, DSLR 5300; 7, Tripod for long exposure photography. Not to scale.

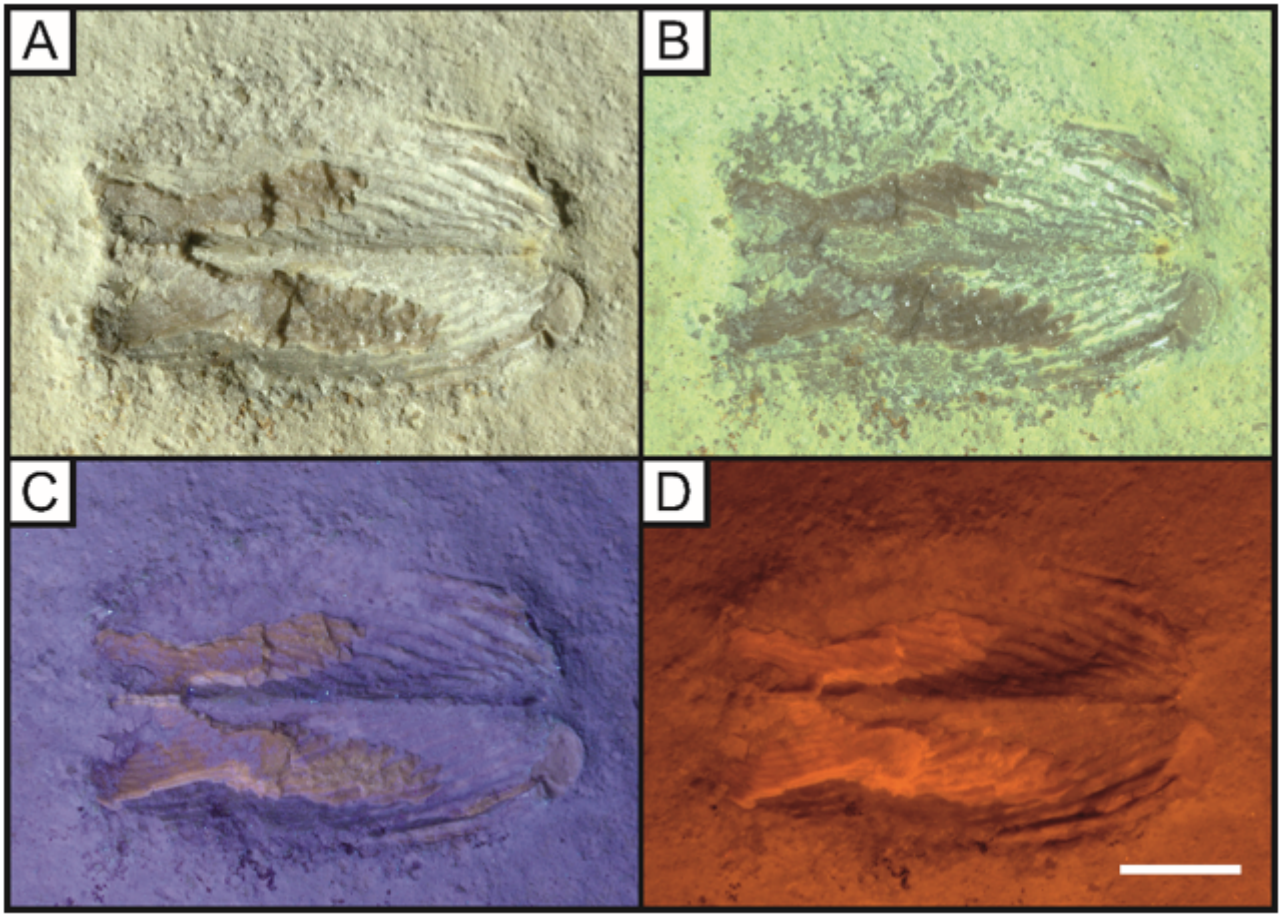

Figure 3

Isolated specimen of Lamellaptychus (LB 1), a genus for ammonite mouthparts not associated with a specific taxon, under white light (A-B), UV (C) and LSF (D). A. Direct white light image differentiating between the brown thick spongy layer and the thin crenulated layer beneath; B, oblique white light casting a shadow on the specimen revealing the full outline; C, ultraviolet light of 365 nm wavelength used to display colour differences between the two layers; D, Increased contrast under LSF using a 532 nm green laser allows the full outline of the original shape to be observed. Scale bar = 10mm.

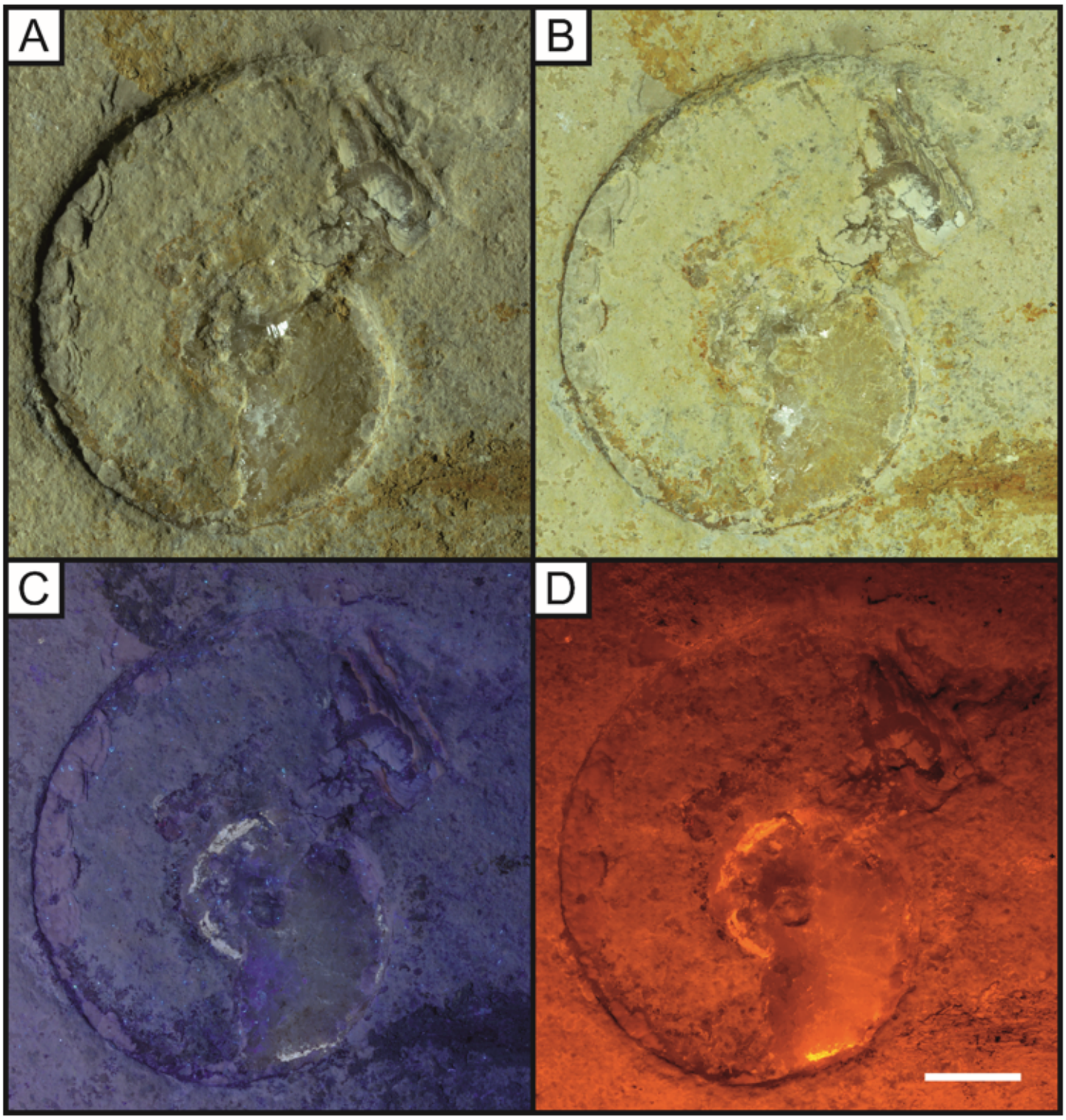

Figure 4

The oppeliid ammonite Neochetoceras bous Oppel, 1863 with a calcified phragmacone, full body chamber outline and preserved aptychi (LB 2). A, oblique white light displaying remnants of the body chamber at the left inside edge; B, UV image displaying the siphuncle, phragmacone and jaw apparatus with colour differences along with possible stomach contents; C, LSF image of Neochetoceras bous

under a 532 nm green laser with phosphatised siphuncle along with a clear boundary between the phragmacone and body chamber unseen in other methods. Scale bar = 10 mm.

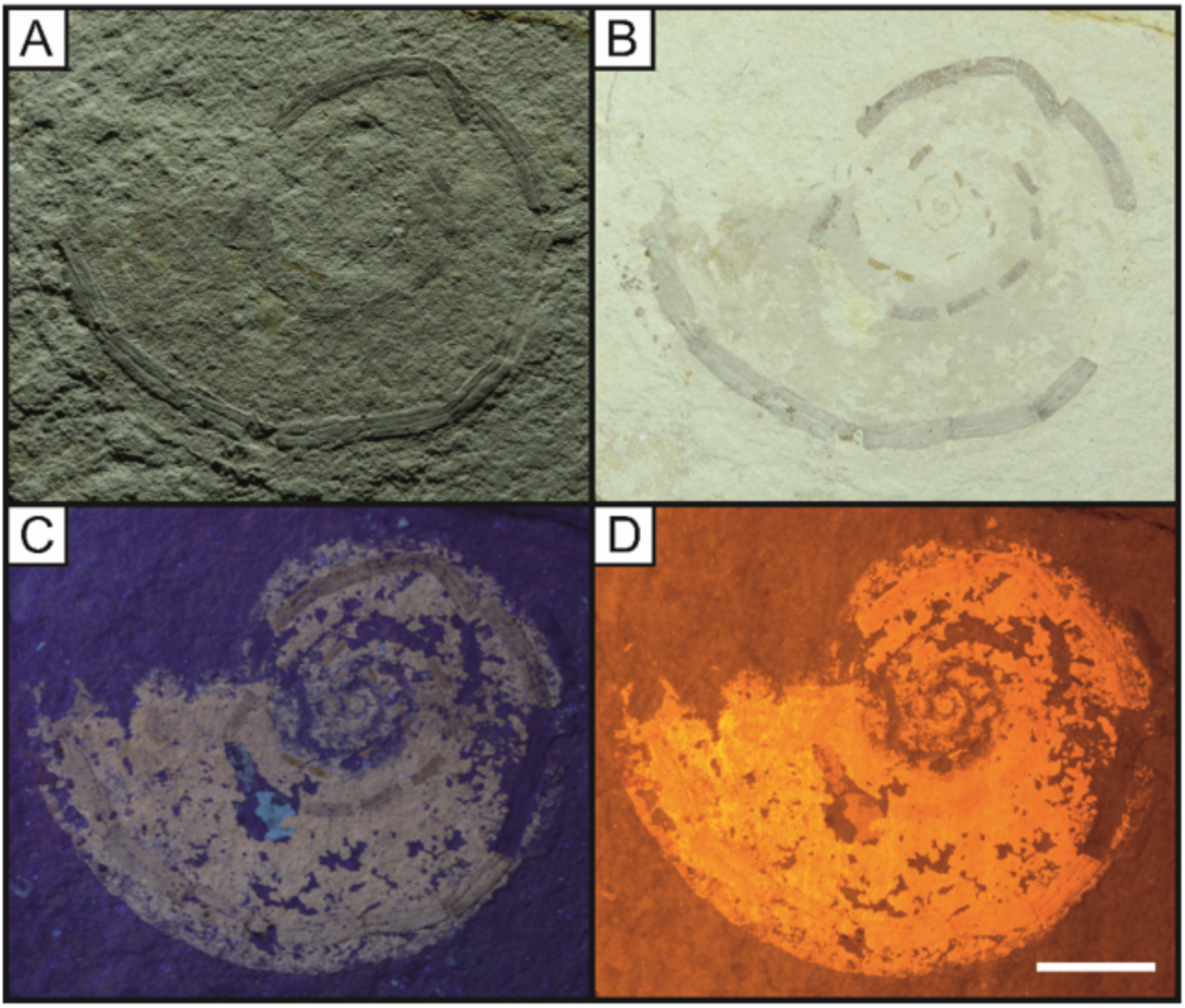

Figure 5

The phragmacone of the oppeliid ammonite Fontannesiella prolithographica (Fontannes) (LB 3) with phosphatised siphuncle under white light (A-B), UV (C), and LSF under 532 nm green laser light (D). Note the colour variation seen under 365 nm UV is not consistent with Fig. 6 and may be because of differential preservation. Scale bar = 10 mm.

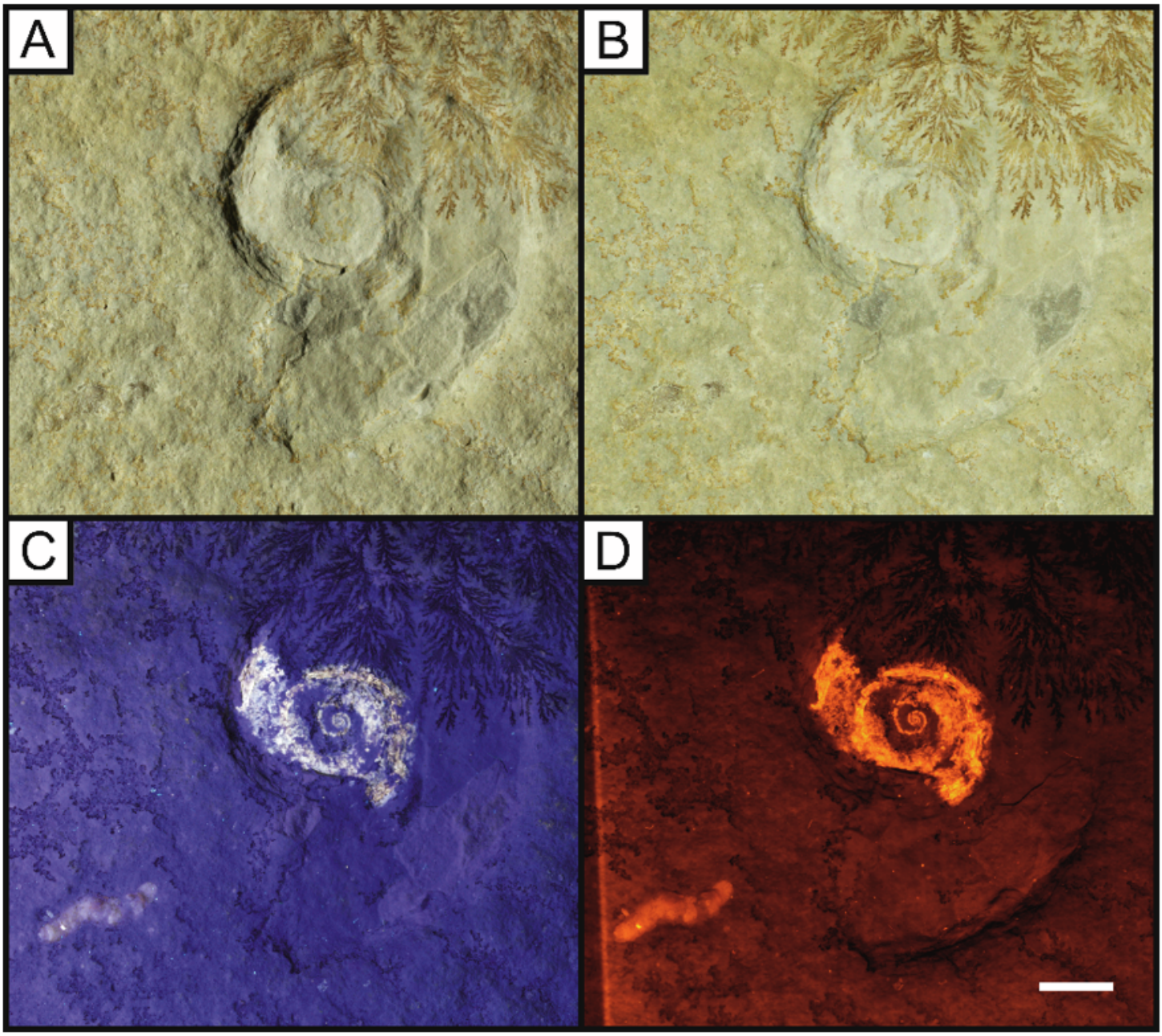

Figure 6

The oppeliid ammonite Neochetoceras sp. with some phragmacone fluorescence and the ammonite coprolite Lumbricaria attributed to LB 4. A, direct white light recording a slight colour difference around the phragmacone and very little evidence of the coprolite; B, oblique white light; C, UV light fluorescing the coprolite, siphuncle and phragmacone; D, LSF displaying full fluorescence of the phragmacone, increasing the observed contrast. Note the brighter siphuncle under 532 nm green laser light in D, allowing for a greater distinction than under UV light seen in C. Scale bar = 10mm.

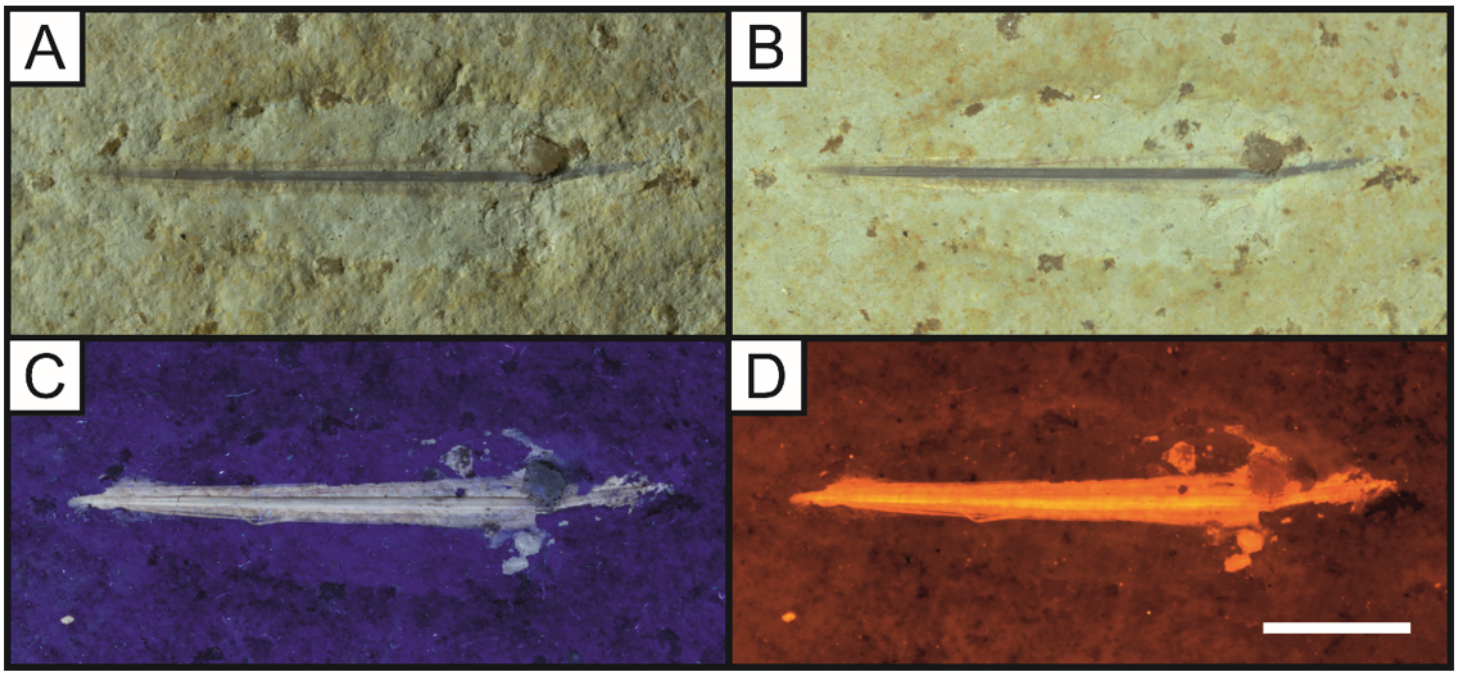

Figure 7

The plesioteuthid squid Plesioteuthis prisca with a fluorescent gladius (LB 5). This squid can be seen under oblique (A) and direct white light (B). 365nm UV light fluoresces the rachis in this specimen, showing that the central rachis is raised (C). LSF using the 532 nm laser fluoresces this gladius at different levels with the central vane picked out through its higher fluorescence. Scale bar = 10mm.

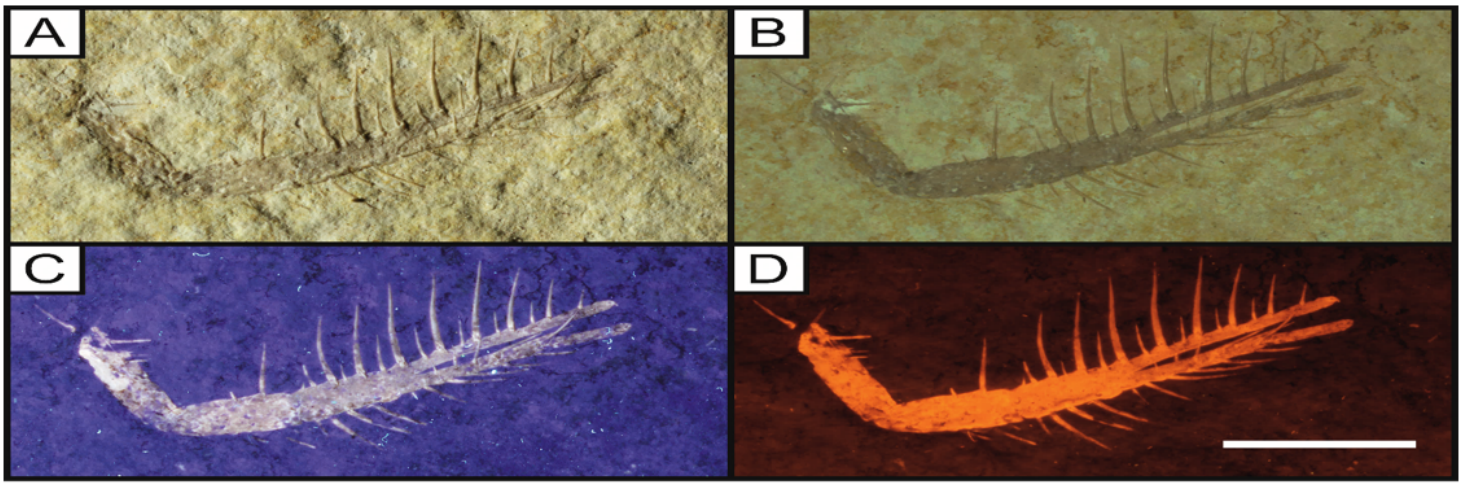

Figure 8

An isolated appendage of the fossil prawn Aeger tipularius under different lighting conditions (A-D) (LB 6). A, oblique white light image, casting shadows on the slight relief present; B, direct white light; C, Same specimen under 365 nm ultraviolet fluorescence, highlighting the specimen from the background and recovering some unseen setae that appear broken; D, Laser-stimulated fluorescence image of the

specimen under 532 nm green laser displaying an improvement over the UV image seen in C with the complete leg revealed along with none of the gaps present under UV. Scale bar = 10mm.

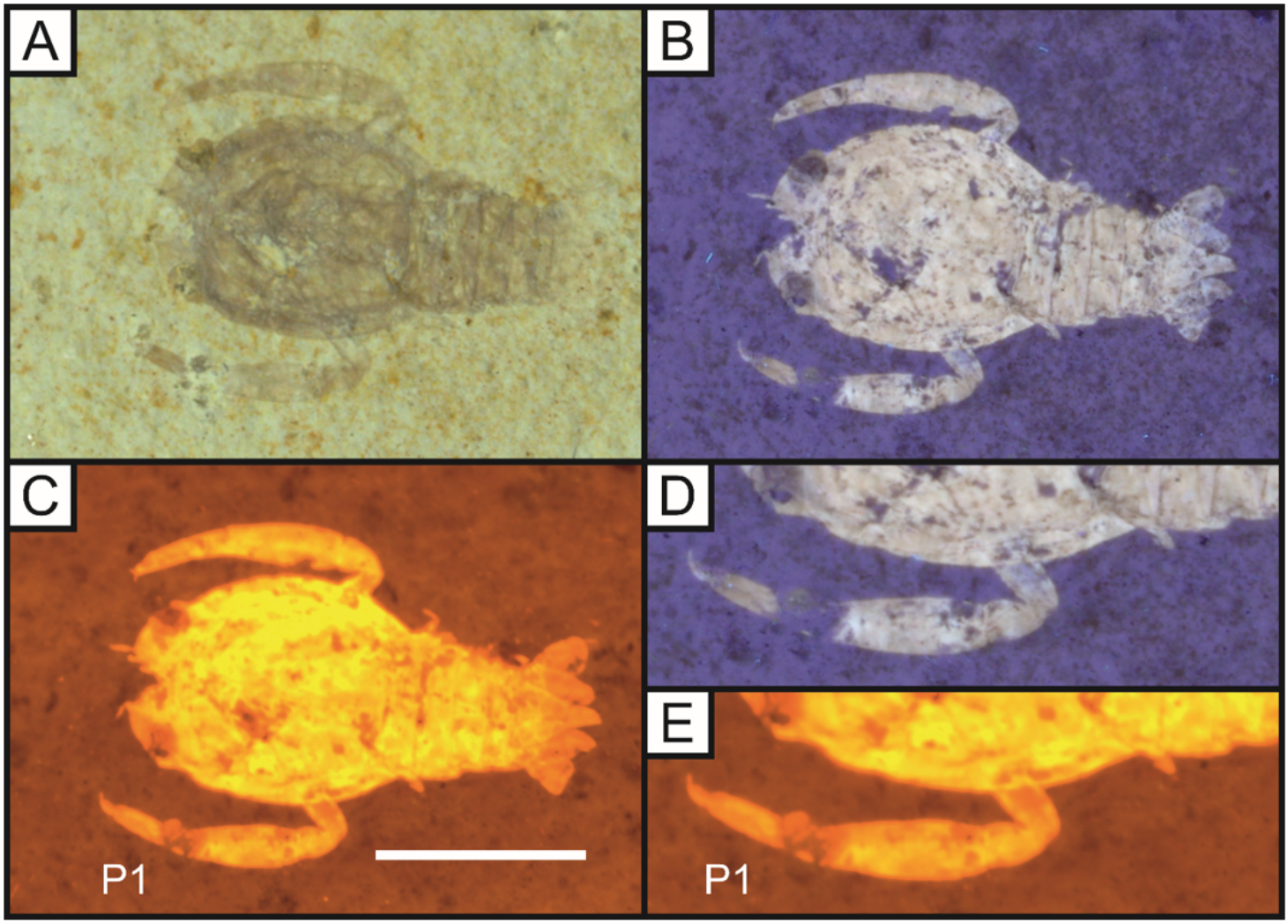

Figure 9

The eryonid crustacean Cycleryon propinquus von Schlotheim, 1822 under white light (A), 365 nm UV (B) and LSF (C) revealing the full outline of the animal under a 532 nm green laser (LB 7). D and E represent comparisons of the fluorescent techniques on the first pereopod (P1). Note the missing section under UV light is revealed through the subsurface illumination of LSF. Scale represents 1cm. D and E magnified x1.5.

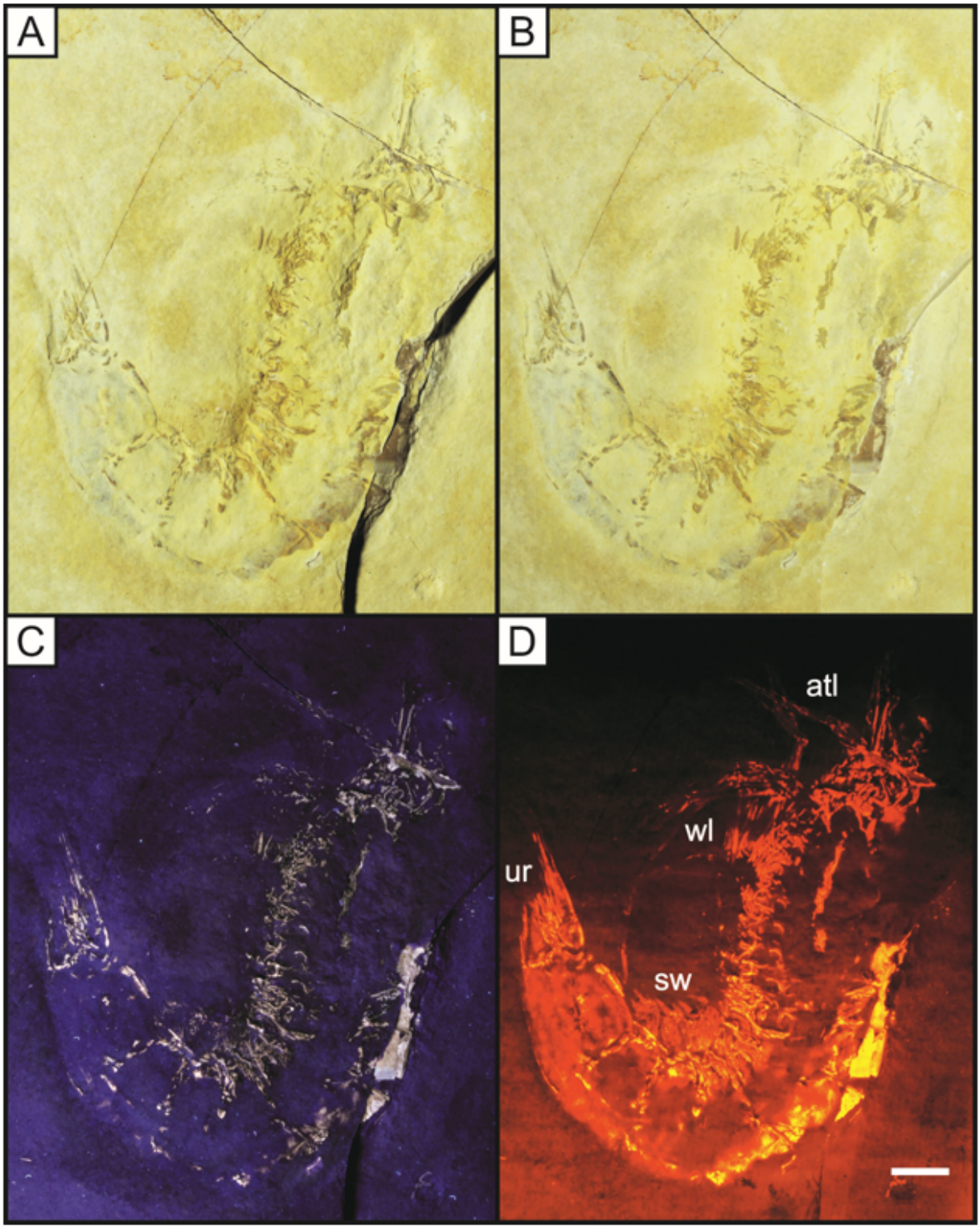

Figure 10

Complete fossil of the penaeid shrimp Antrimpos speciosus Münster, 1839 (LB 8) under different lighting conditions; A, oblique white light showing the split rock revealing the original exoskeleton; B, direct white light; C, UV fluorescence increases the contrast with the background by illuminating the specimen and leaving the matrix dark; D, LSF reveals the entire body outline of the animal and this not seen in the white light or UV photographs. Note the antennulae (atl), swimmerets (sw), walking legs (wl) and urostyle (ur)

which were not fully visible in white light. Abbreviations following C. Haug et al. (2009). The green laser wavelength used on this specimen was 532 nm. Scale bar = 10 mm.

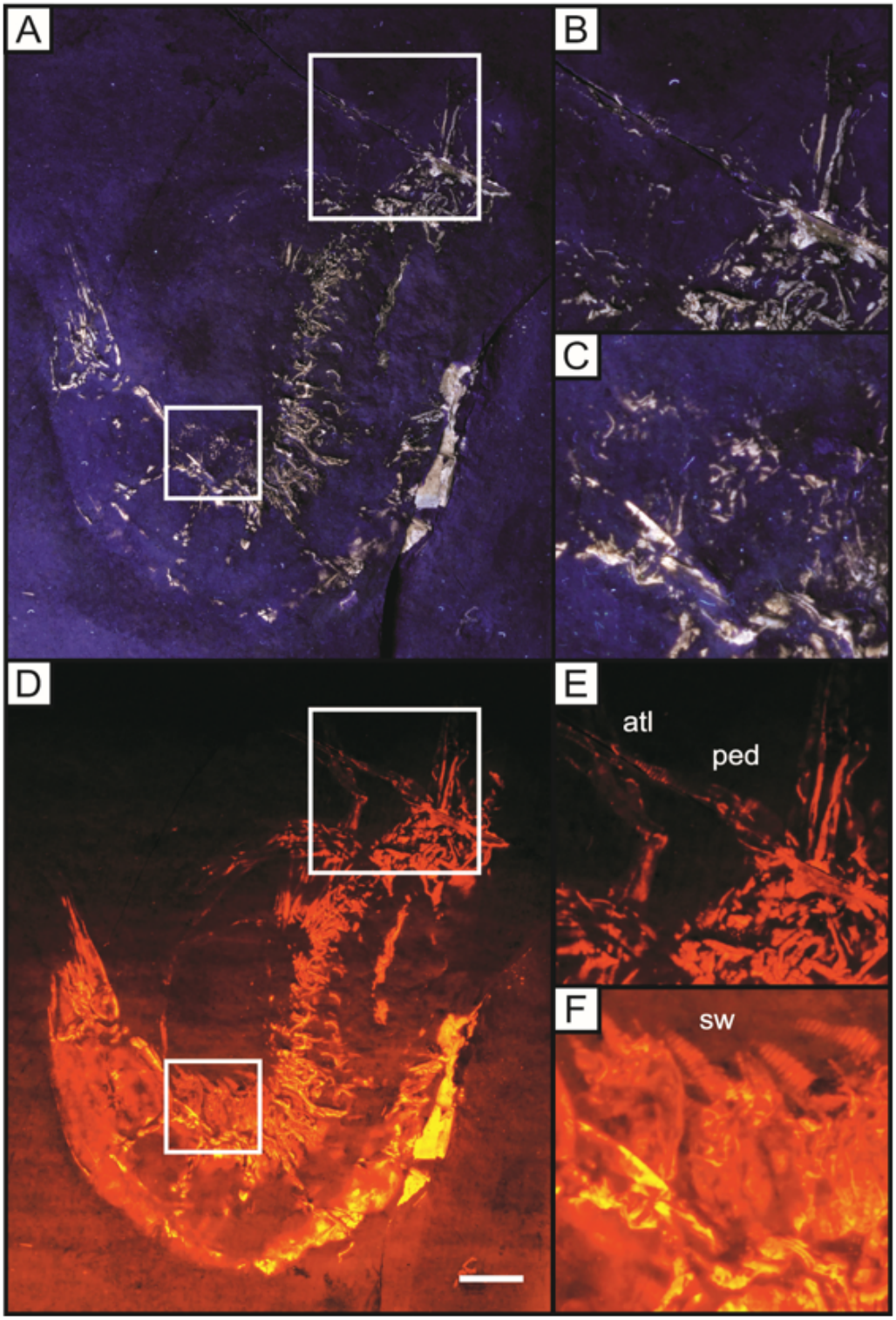

Figure 11

Isolated UV (A-C) and LSF (D-F) images from Fig. 10 highlighting the differences in revealed detail. B and E are UV and LSF images of the revealed antennae with clear segmentation visible under LSF. C and F highlight the swimmerets that are fully revealed under LSF with full segmentation. Abbreviations as

above with the addition of the antennular peduncle (ped) from Audo and Charbonnier (2012). Scale bar = 10mm. B and E magnified x2 and C and F magnified x3.6.

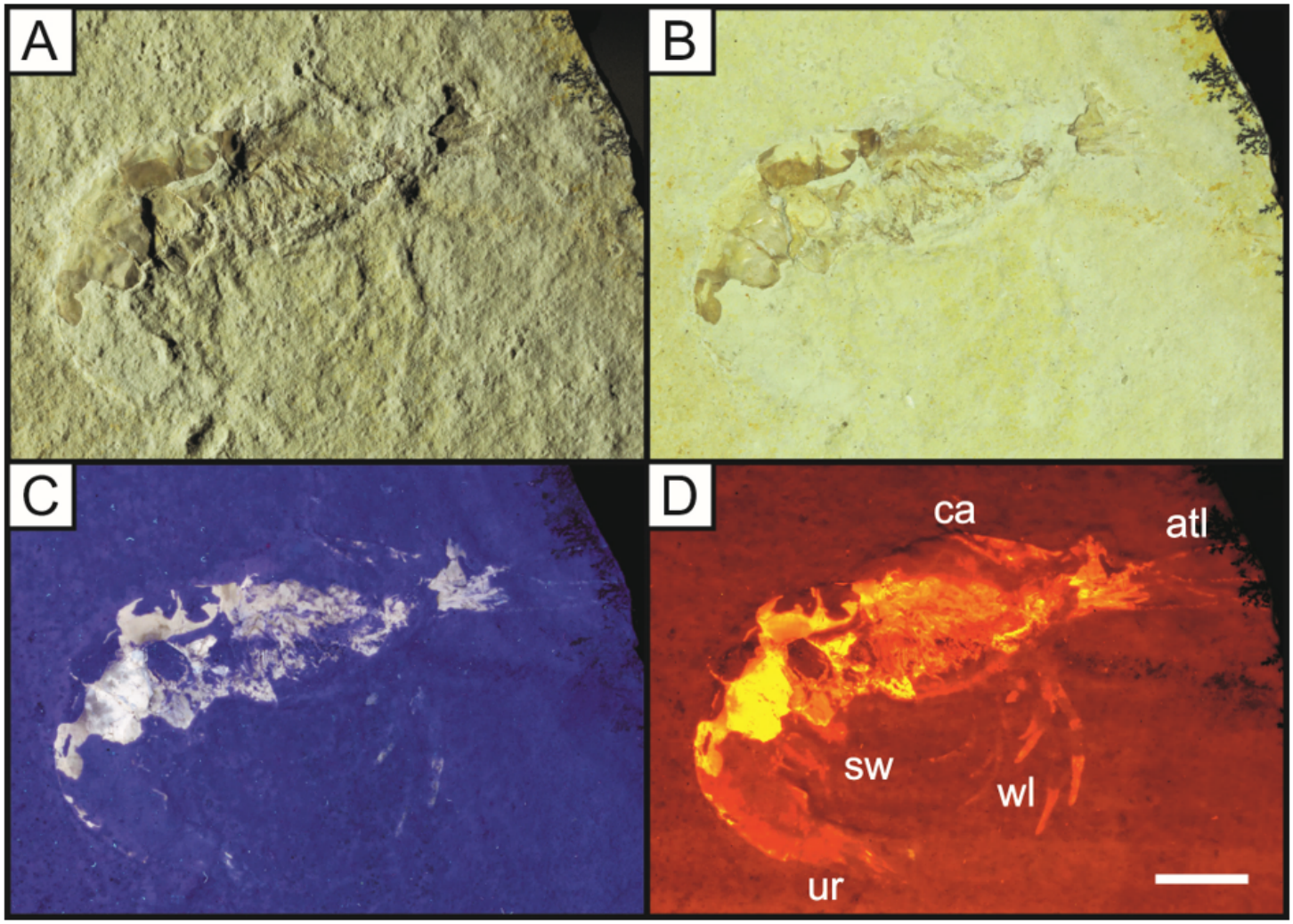

Figure 12

Specimen LB 9 of the caridean shrimp Alcmonacaris winkleri under oblique white light (A), direct white light (B), UV fluorescence (C) and LSF (D). Notice the faint outline under UV is enhanced through LSF to reveal the full animal, allowing the fossil to be labelled. Scale = 10mm. The features revealed use the same abbreviations as Fig. 9 with the addition of the carapace (ca). Abbreviations following C. Haug et al. (2009). The LSF wavelength used was 532 nm.

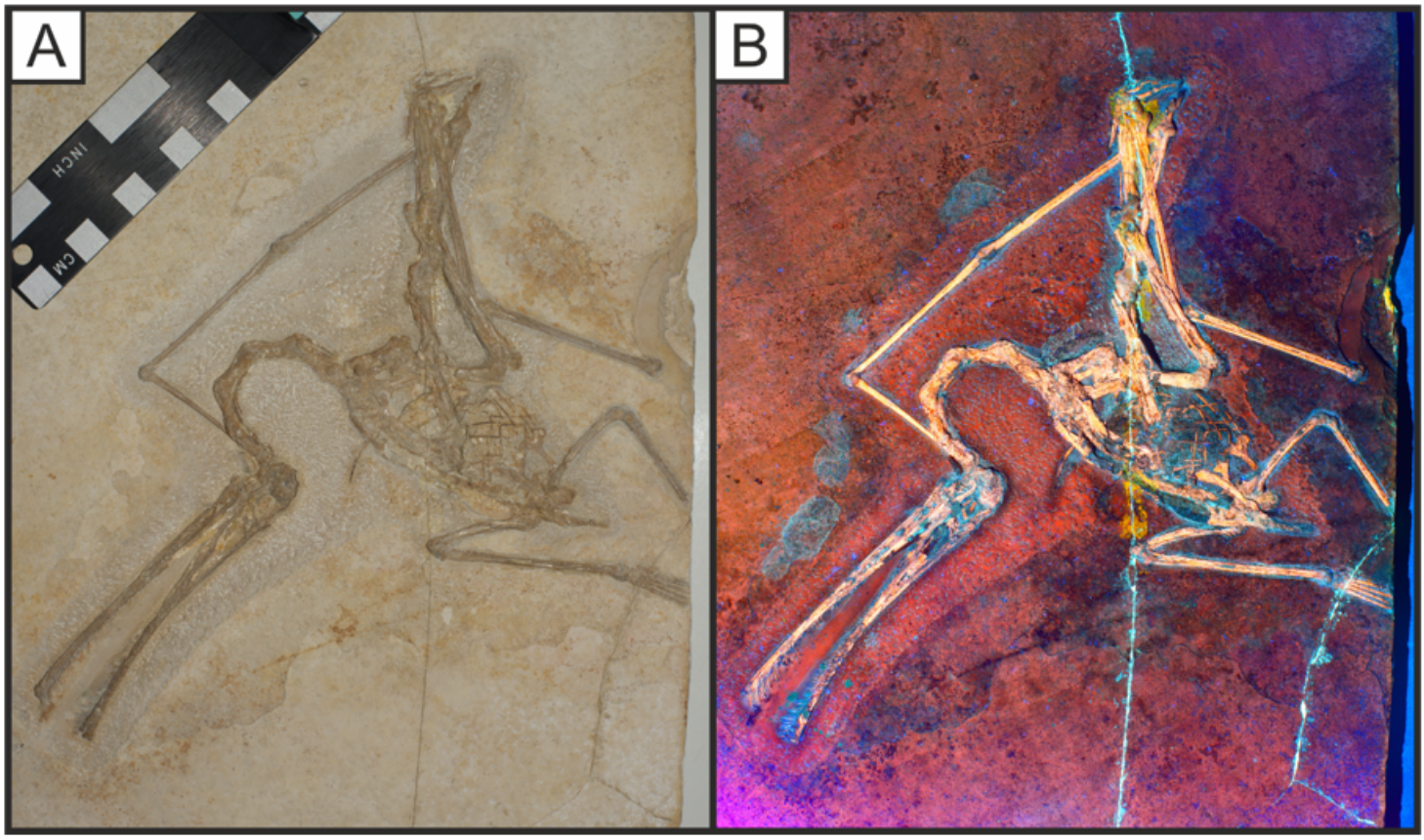

Figure 13

Specimen SNSB-BSPG 1935 I 24 of the pterodactyloid pterosaur Ctenochasma gracile under white light (A) and LSF (B). This individual is fully articulated with a blue fluorescent soft tissue body outline and blue cartilage between the light orange bones. A 405 nm blue laser was used to fluoresce this specimen.

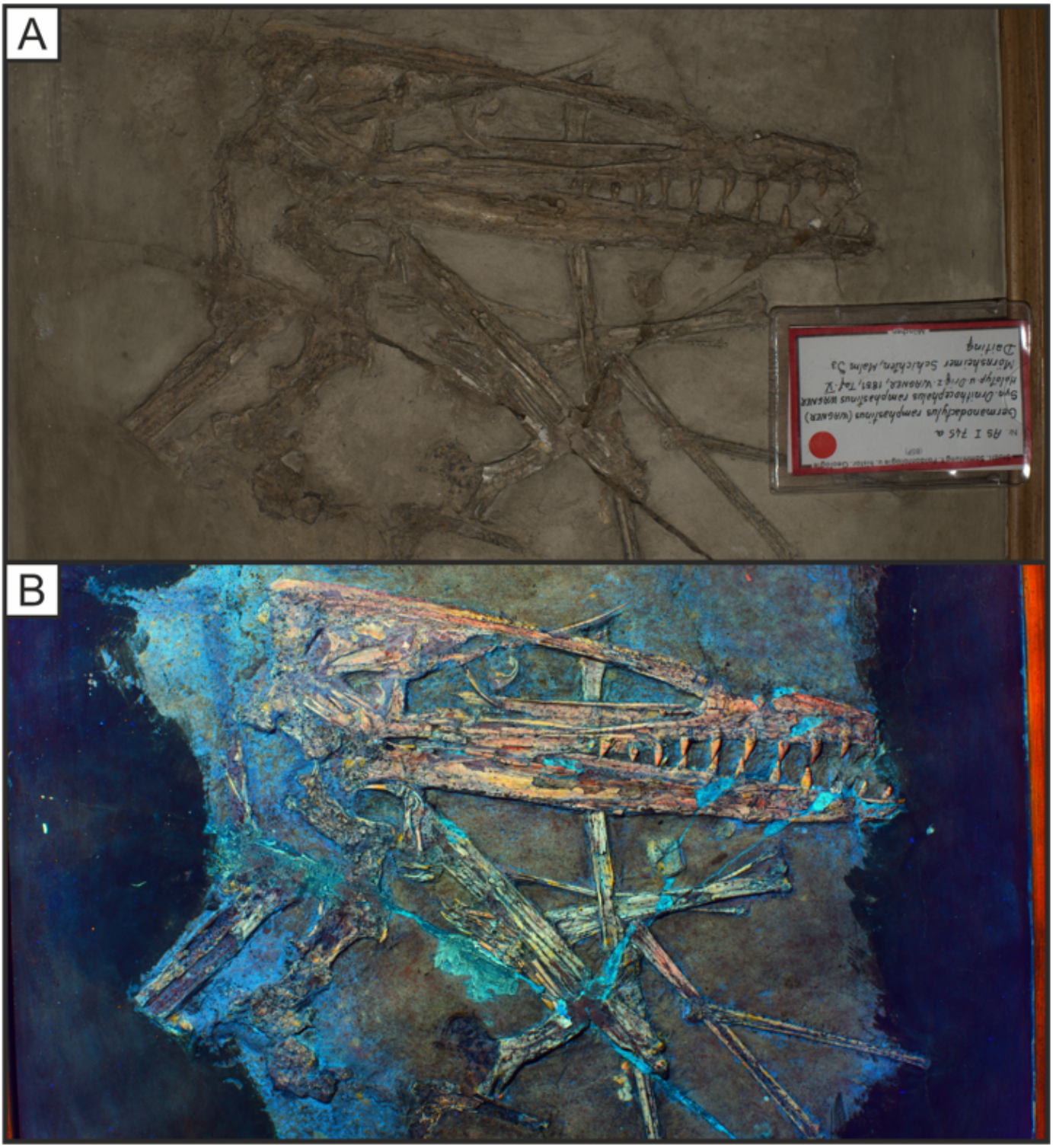

Figure 14

Specimen SNSB-BSPG AS I 745a of the pterodactyloid pterosaur Germanodactylus rhamphastinus under white light (A) and LSF (B). The skull and upper torso have an increased contrast under LSF through a 405 nm blue laser, separating the specimen from the surrounding matrix. Specimen badge measures 5cm.

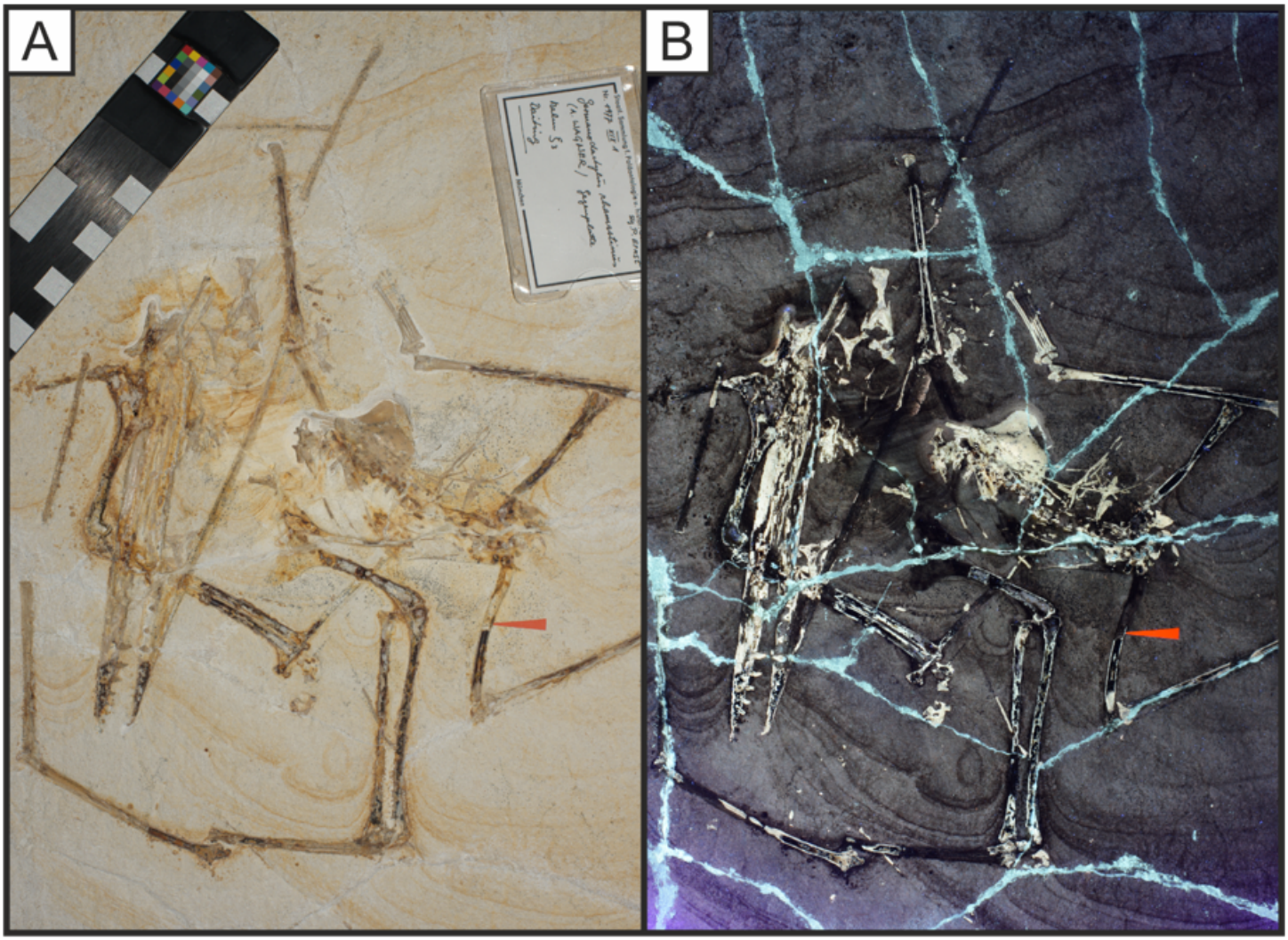

Figure 15

Specimen SNSB-BSPG 1977 XIX 1 of the pterodactyloid pterosaur Germanodactylus rhamphastinus on a counterplate slab under white light (A) and LSF (B). The counterplate slab has some missing bone material where it remains dark under LSF. A 405 nm blue laser was used to carry out LSF and fluoresces any preserved bone material.

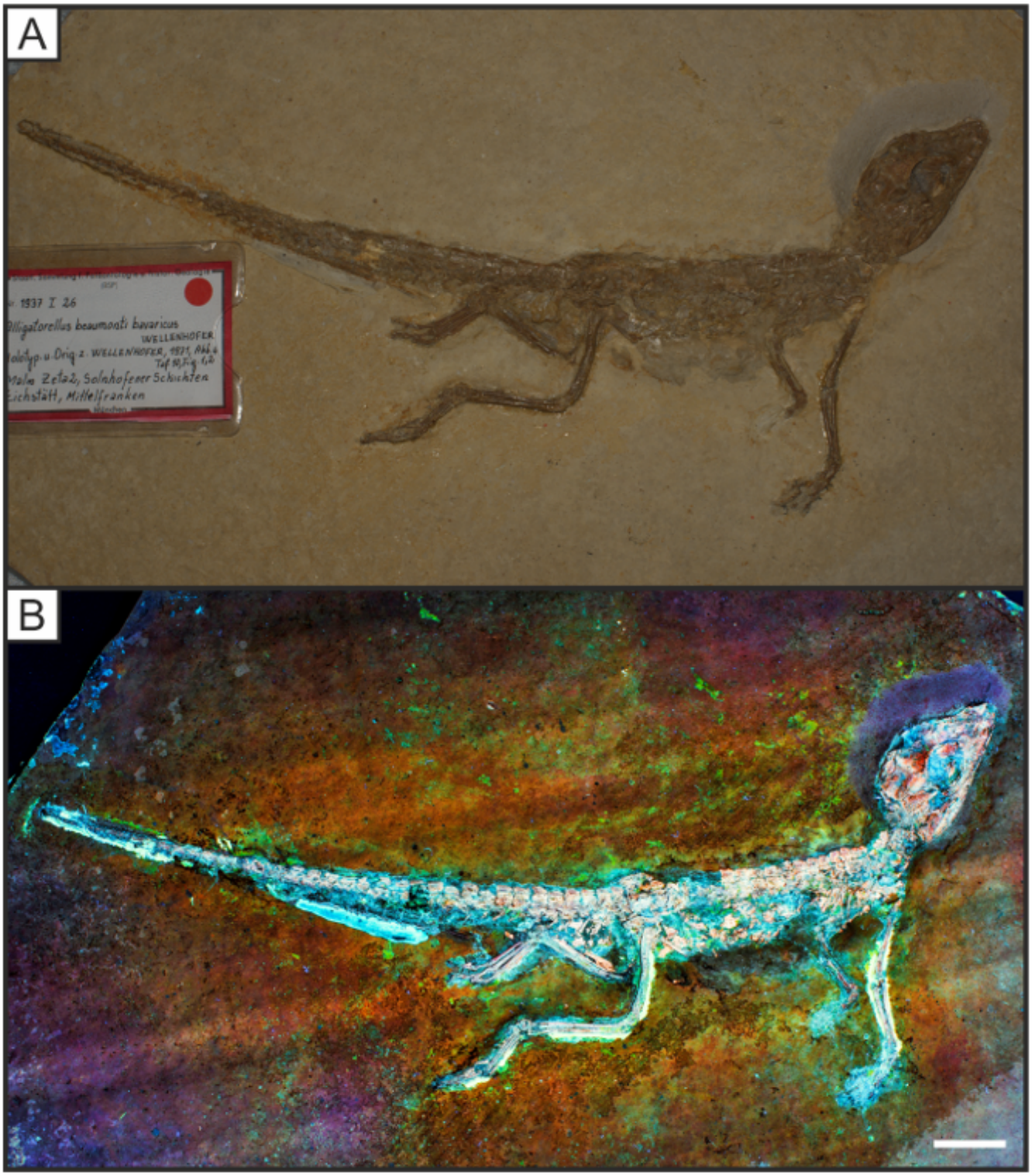

Figure 16

Specimen SNSB-BSPG 1937 I 27 of the atoposaurid crocodyliform Alligatorellus beaumonti bavaricus under white light (A) and LSF (B). The colour patterning makes clear distinction possibly between the skeleton and osteoderms and the surrounding soft tissues. Note the brightly fluorescing soft tissues at the base of the tail, possibly phosphatised remnants of muscle tissue. LSF was carried out using a 405 nm blue laser. Scale represents 2cm.

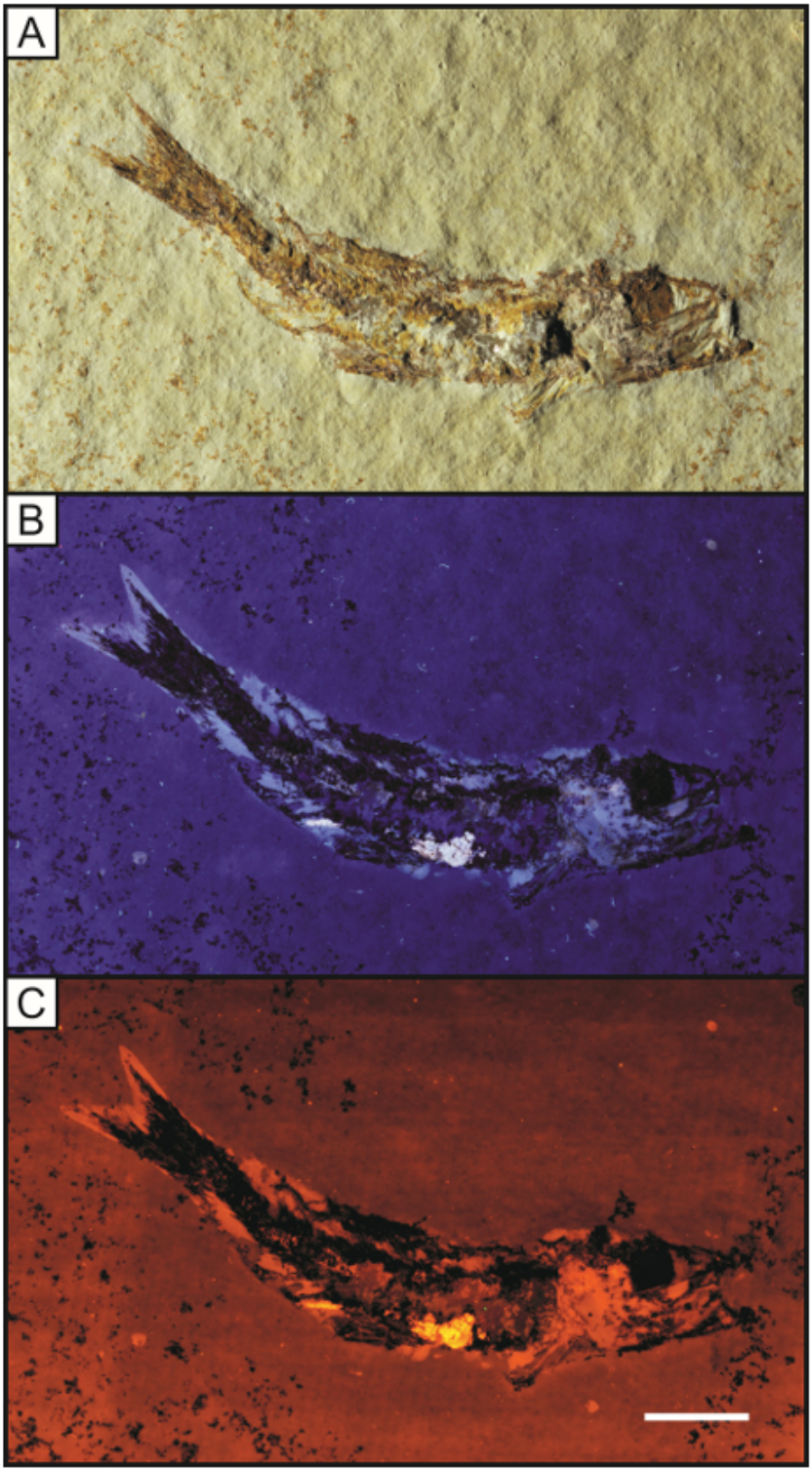

Figure 17

A specimen of the teleost fish Leptolepides sprattiformes Blainville, 1818 (LB 10), under white light (A), UV fluorescence (B) and LSF (C). Not the completed soft tissue outline that is brighter than the ossified material. Gut contents fluoresce brightly at the centre of the body cavity along with a coprolite illuminated at the posterior. The laser used on this specimen was a 532 nm green laser. Scale = 10 mm.

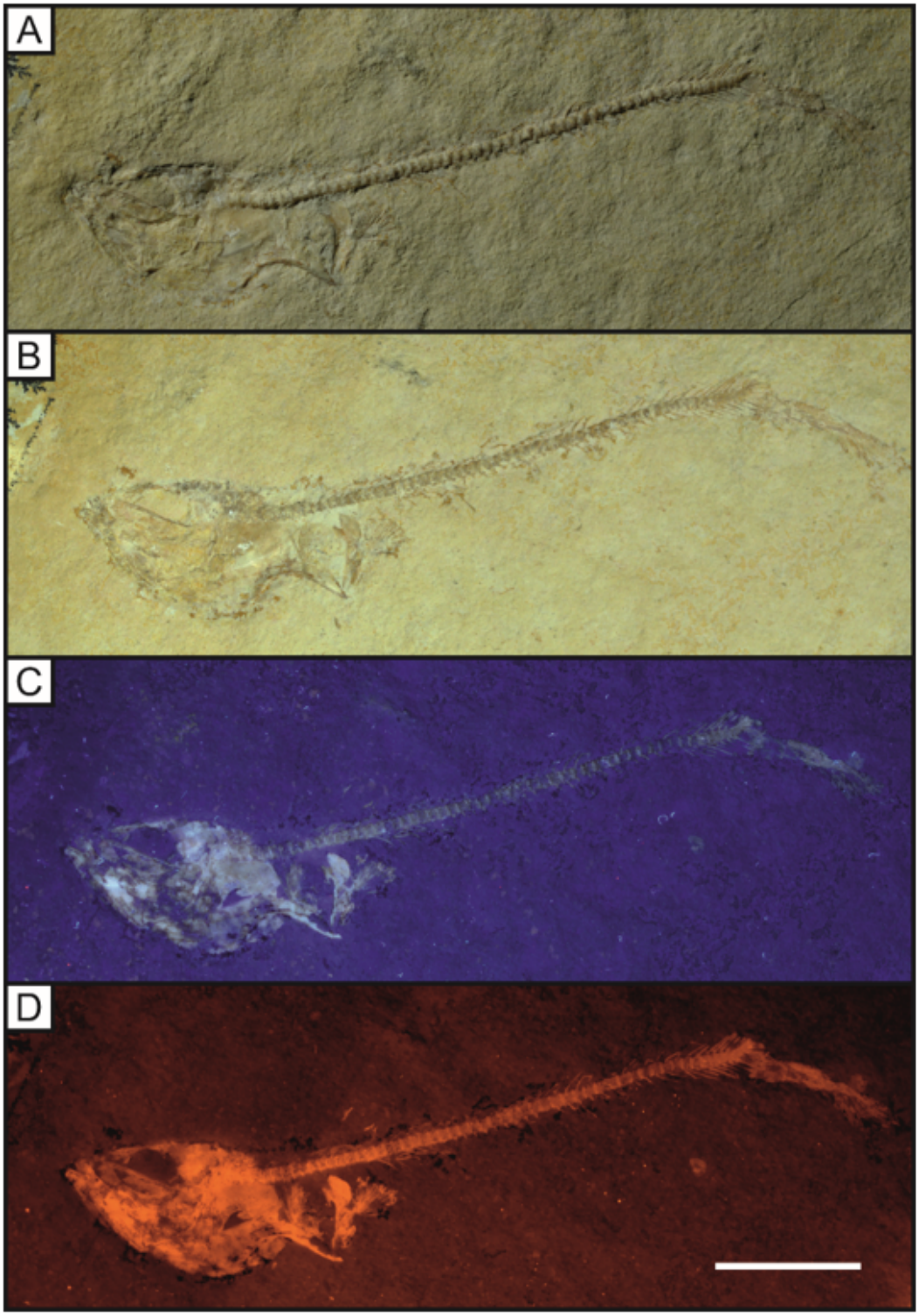

Figure 18

A near complete specimen of the salmoniform fish Orthogonikleithrus hoelli, lacking the dorsal section of caudal fin (LB 11). A, oblique white light photograph showing a complete vertebral column and faint skull and caudal fin elements; B, direct white light image; C, UV fluorescence highlighting the bones of the skull along with the pectoral fin; C, enhanced fluorescence from B showing the caudal fin is incomplete along with fluorescing the entire skull. LSF was carried out with a 532 nm green laser. Scale bar = 20 mm.

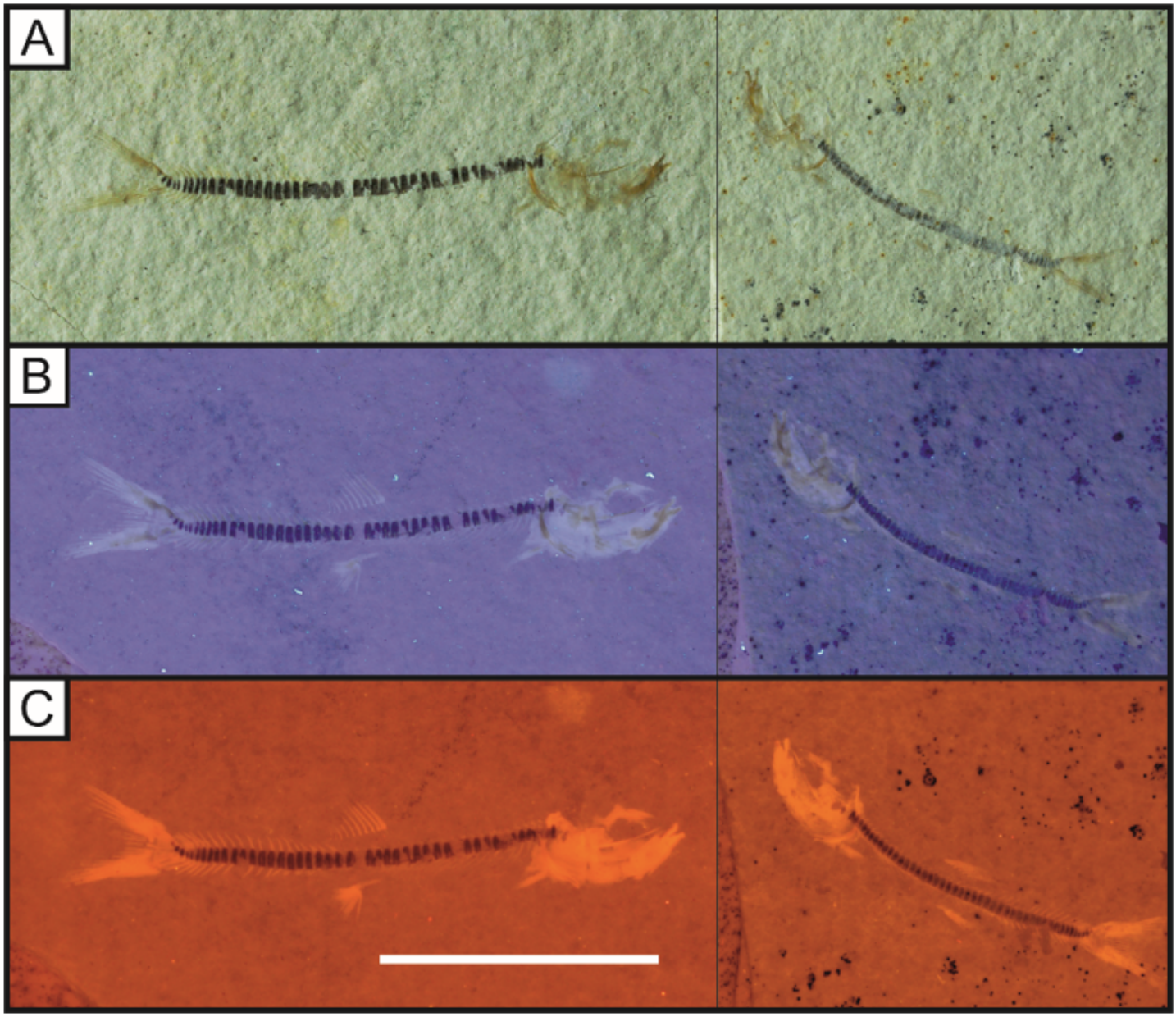

Figure 19

Two small specimens of the salmoniform fish Orthogonikleithrus hoelli on the same slab (LB 12) under different light conditions. A, oblique white light photograph with a dark vertebral column and lighter skull and fins present; B, UV photograph with complete skull and tail revealed. Dorsal and pelvic fins are also revealed through fluorescence with illumination from the left; C, LSF image revealing the entire dorsal and pelvic fins on the right specimen that are faint under UV. Note the erect position of the dorsal and pelvic fins on the left and relaxed position on the right. A 532 nm green laser was used to carry out LSF. Scale bar = 10mm.

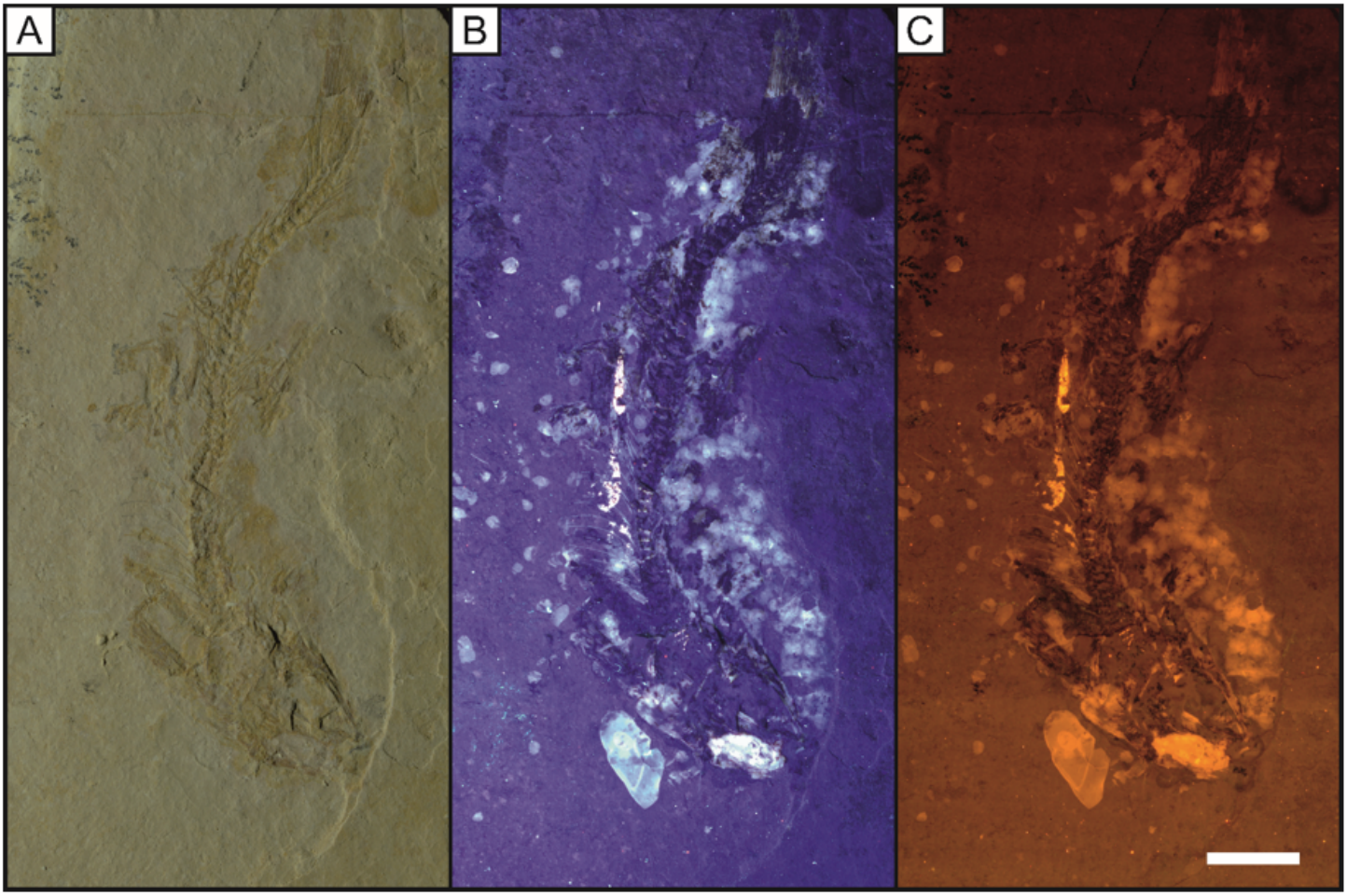

Figure 20

Specimen LB 13 of the extinct bulldog fish Allothrissops salmoneus (Blainville, 1818) under white light (A), UV (B) and LSF (C) conditions. The fluorescence around the articulated skeleton reveals loose scales along with gular plates and gut contents. A 532 nm green laser was used to carry out LSF. Scale bar = 10 mm.